Parametric Channel Model Estimation for Large Intelligent Surface-Based Transceiver-assisted Communication System

A Project Report submitted by

by

Debamita Ghosh

Under the guidance of

Prof. Manjesh Kumar Hanawal
Department of IEOR, IIT Bombay
&
Prof. Nikola Zlatanov
Department of ECSE, Monash University

IITB-Monash Research Academy
Indian Institute of Technology Bombay

April 7, 2022

Declaration

I declare that this written submission represents my ideas in my own words and where other's ideas or words have been included, I have adequately cited and referenced the original sources. I also declare that I have adhered to all principles of academic honesty and integrity and have not misrepresented or fabricated or falsified idea/data/fact/source in my submission. I understand that any violation of the above will be cause for disciplinary action by the Institute and can also evoke penal action from the sources which have thus not been properly cited or from whom proper permission has not been taken when needed.

In keeping with the general practice of reporting scientific observations, due acknowledgement has been made wherever work described here has been based upon the work of other investigators. Any oversight due to error of judgement is regretted.

Date: April 7, 2022
Place: Mumbai

Debamita Ghosh
194194001

Acknowledgement

There are many individuals who have played an important role in my success. First and foremost my sincere appreciation and thanks goes to my advisors Prof. Manjesh Kr. Hanawal, Department of Industrial Engineering and Operations Research (IEOR), IIT Bombay, India and Prof. Nikola Zlatanov, Department of Electrical and Computer Systems Engineering (ECSE) at Monash University in Melbourne, Australia. Their generous support and guidance with immense patience, motivation, and knowledge had guided me to pursue my research in machine learning for next-generation wireless communications. I could not have imagined having a better advisor and mentor for my PhD study. I am also thankful to Mojtaba Ghermezcheshmeh, PhD scholar, Monash University for his constant co-operation and extended hand of support in understanding the problem statement.

I am also thankful to IITB-Monash Research Academy, IIT Bombay for providing me the opportunity and facilities in finding innovative solutions to research questions across specialist areas of growing global significance in Wireless Communication. I am also thankful for the support of my family and friends who had made this journey possible through significant amount of support and sacrifice.

Most of the report's material is focused on Tor Lattimore and Csaba Szepesvari's book "Bandit Algorithms", Sébastien Bubeck and Nicolo Cesa-Bianchi's book "Regret Analysis of Stochastic and Nonstochastic Multi-Armed Bandit Problems", and two other books on Concentration Inequalities as - "Concentration of Measure for the Analysis of Randomized Algorithms" by Devdatt P. Dubhashi and Alessandro Panconesi and "Concentration Inequalities: A Nonasymptotic Theory of Independence" by S. Boucheron, G. Lugosi and P.Massart.

Abstract

Next generation communication networks promise to enable connectivity for all devices so that they can talk to each other and exchange information all the time. This has given rise to concepts like the Internet of things (IoT). IoT is a collection of interrelated computing devices, mechanical and digital machines, supplied with unique identifiers (UIDs), and capable of sharing data over a network. IoT implementations are often divided into consumers (such as smart home, elderly care), commercial (such as healthcare, transportation), industrial (such as manufacturing, agriculture), and utility spaces (such as energy management, environmental monitoring). Previously, our work focused on two main issues of RF-EHN, i.e., "fairness" and "energy-efficiency" of the wireless communication system. We proposed a design RF Energy harvesting network and implement learning algorithms for RF energy harvesting that will improve the RF Energy harvesting and will implement them in practical scenarios. We model our problem as multi-armed bandits and proposed upper confidence bound based algorithm that solves the practical challenges faced by RF-RHN with performance guarantees. We also validated the performance of the proposed algorithm by numerical simulations.

However, the number of connected mobile devices and the amount of data traffic through these devices are expected to grow many-fold in future communication networks. To support the scale of this huge data traffic, more and more base stations and wireless terminals are required to be deployed in existing networks. Nevertheless, practically deploying a large number of base stations having massive antenna arrays will substantially increase the hardware cost and power consumption of the network. More recently, Reconfigurable Intelligent Surfaces (RIS)/ Intelligent Reflecting Surfaces (IRS)/ Large Intelligent Surfaces (LIS) aided communication has emerged as a promising reflective-radio technology for next-generation networks capable of fulfilling the demand of high spectral efficiency. It is also considered to be a cost effective and energy efficient solution. A typical LIS consists of a planar array having a large number of reflecting metamaterial elements (e.g., low-cost printed dipoles), each of which could act as a phase shift. In particular, the passive or reflective-radio elements of the LIS interact with incident electromagnetic waves and reflect them towards the receiver. More importantly, it enables the system to construct a programmable wireless environment suitable for communication.

A promising approach for enhancing the coverage and rate of wireless communication systems is the large intelligent surface-based transceiver (LISBT), which uses a spatially continuous surface for signal transmission and receiving. Accurate channel state information (CSI) in LISBT-assisted wireless communication systems is critical for achieving these goals. In this paper, we

propose a channel estimation scheme based on the physical parameters of the system. that requires only five pilot signals to perfectly estimate the channel parameters assuming there is no noise at the receiver. In the presence of noise, we propose an iterative estimation algorithm that decreases the channel estimation error due to noise. The proposed scheme's training overhead and computational cost do not grow with the number of antennas, unlike previous work on enormous multiple-input multiple-output (MIMO). The channel estimate scheme based on the physical properties of the Large intelligent surface-based transceiver (LISBT)-assisted wireless communication systems is the subject of our future study.

Contents

List of Abbreviations

IOT	Internet of Things
LISBT	Large Intelligent Surface-Based Transceiver
RIS	Reconfigurable Intelligent Surfaces
IRS	Intelligent Reflecting Surfaces
LIS	Large Intelligent Surfaces
MIMO	Multiple-Input Multiple-Output
WSN	Wireless Sensor Networks
RF-EHN	RF Energy Harvesting Network
CSI	Channel State Information
MDP	Markov Decision Process
DP	Dynamic Programming
MAB	Multi-Armed Bandits
UCB	Upper Confidence Bounds

List of Figures

Chapter 1

Introduction

Future wireless networks, namely beyond fifth generation (5G) and sixth generation (6G), are required to support massive numbers of users with increasingly demanding spectrum resources, higher data rates, but with lower latency. However, severe path-loss, atmospheric absorption, human blockage, and other environmental obstruction are key challenges for enabling beyong 5G wireless communication. Signal deterioration is perhaps one of the major concerns in millimeter wave and in the forthcoming TeraHertz (THz) communications [17], [9]. The goals of sixth-generation (6G) wireless communication systems are expected to be transformative and revolutionary encompassing applications like data-driven, instantaneous, ultra-massive, and ubiquitous wireless connectivity, as well as connected intelligence [11], [13]. Future 6G wireless communication systems are expected to realize an intelligent and software reconfigurable paradigm, where all parts of device hardware will adapt to the changes of the wireless environment. Therefore, new transmission technologies are needed in order to support these new applications and services. Moreover, since the beamforming gain of massive MIMO increases with the number of antennas, it would be highly desirable to have large number of antennas (extremely large number of sub-wavelength phase-shifting elements), which is not feasible in reality. In this direction, large intelligent surfaces (LISs) are introduced to go beyond massive MIMO systems.

The LISs have emerged as a promising technology for packing a massive number of sub-wavelength phase-shifting elements in a very small area that could generate narrow beams with high beamforming gains [5], [8]. The LIS can be used as an intelligent reflecting surface (IRS) or an LIS-based transceiver (LISBT). When an IRS is placed between the base stations (BS) and the user, it can manipulate the incident electromagnetic (EM) wave impinging on it and reflects it towards the user [19]. Similarly, an IRS that has a line-of-sight (LoS) link with the BS and the user, can intelligently overcome the obstacle caused by any blockage in the direct link

between the BS and the user. In contrast to the IRS that has attracted considerable research attention, the application of LIS as a LISBT has lacked behind in research outputs. Therefore, in this paper we focus on LISBT.

The LISBTs can be represented as an extension of massive MIMO with discrete antenna array to continuous reflecting surface, and can also exploit the advantages of LIS based on radiating elements to control the analog beamforming for transmission and reception [18], cf. Fig. 1.1. The existing research works have verified the effect of LISBTs on enhancing the communication performance in various scenarios under the assumption of the availability of perfect channel state information (CSI) [21]. However, the acquisition of accurate CSI is a fundamental and challenging task in practice in order to estimate channel coefficient of LISBT-assisted wireless communication system. Due to large number of phase-shifting elements in the LISBT, estimation of the entries of channel matrix will impose substantial training overhead and high computational cost. However, due to the sparse nature of channels in mmWave and THz frequency bands, the parameters of the dominant paths, e.g., angle of arrival (AoA), angle of departure (AoD), and path gain, can be estimated to reduce the training overhead [21]. This motivated us to propose a channel estimation scheme for the LISBT-assisted wireless communication system based on the path parameters with minimum number of pilot signals.

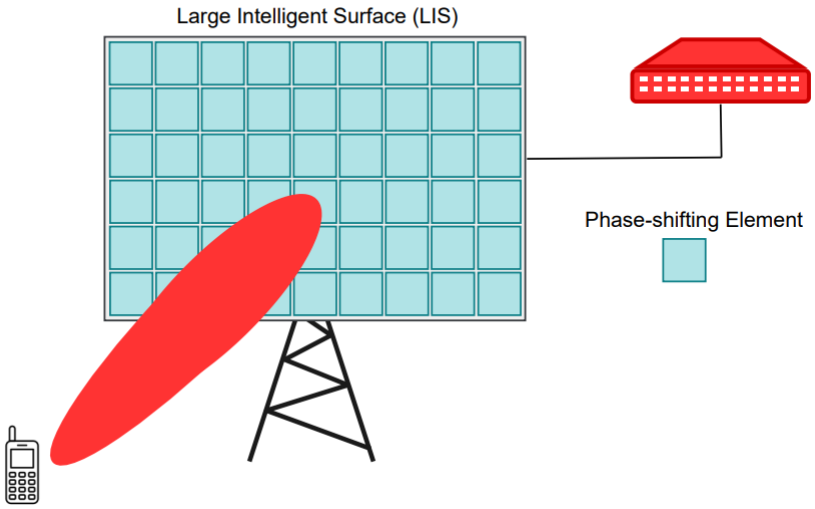

Figure 1.1: The LISBT consisting of a massive number of phase-shifting elements, transmits/receives the signal with high beamforming gain towards/from the user [6].

1.1 Related Works

LISBT-assisted wireless communication system is introduced recently as the application of the LIS. Thereby, the problem of channel estimation of LISBT is a new research area. The existing literature proposes a variety of channel estimation schemes have been proposed in the massive MIMO communication systems to estimate the path parameters, including exhaustive search [4], hierarchical search [21], [3], and compressed sensing (CS) [3]. Even though the exhaustive search is a straight forward method to search exhaustively the best pair of AoA and AoD amongst the all possible anugular directions between transmitter and receiver, the training overhead of the exhaustive search is prohibitively high, especially when a large number of antennas generates narrow beams in the mmWave and THz frequency bands. As an improvement of the exhaustive search the authors proposed the hierarchical search based on a predefined codebook, where in the first stage of the hierarchical search, the codewords with larger beam widths are used to scan the entire angular domain, and, in the second stage, codewords with narrower beam widths are used to scan only a specific range obtained at the first stage. Turning off some antennas is not a good approach since the reduced array gain has an undesirable effect on the performance [22]. In [3], the author proposes a beam training method based on dynamic hierarchical codebook to estimate the mmWave massive MIMO channel with multi-path components. However, the accuracy of the hierarchical search is limited by the codebook size. Moreover, all these hierarchical schemes may incur high training overhead and system latency because they require non-trivial coordination among the transmitter and the receiver. It is shown that CS is also an attractive approach to formulate the channel estimation problem as a sparse signal recovery problem [3]. In the CS-based channel estimation, first a set of random training sequences is used to measure the channel, and then a sparse recovery algorithm is employed to obtain the path parameters. Some proposed CS-based channel estimation schemes have trade-off between accuracy of estimation and training overhead that impacts the computational costs.

Some literature studied the user localization problem where the location of the user is determined by its distance from the BS and the elevation and azimuth AoD. Due to the strong line-of-sight path common to mmWave channels, the path parameters are relied on the physical location of the user [20]. Thereby, the channel estimation problem and user localization are highly correlated [23]. Different form studies in localization problem, we circumvent the estimation of distance to obtain close form solution for channel estimation problem.

In the paper [6], the authors have obtained the optimal phase shifts for all phase-shifting elements by estimating only three parameters, i.e., the distance from the LISBT to the user, the elevation and azimuth AoD, of the parametric channel model in the far-field. But in practice it is impossible to estimate the

distance of the user from the LISBT very precisely. Therefore, they simplified further the LISBT-user channel for the far-field region of the LISBT to overcome the difficulty in estimating of the distance parameter. Moreover, the simplified model requires only two parameters instead of three. They also proposed an efficient scheme to obtain the unknown parameters based on the far-field channel model. The proposed scheme requires only five pilots in order to perfectly estimate the unknown parameters for the case of without receiver noise. In the case with receiver noise, they proposed an iterative algorithm based on the proposed scheme to estimate the unknown parameters. Since the performance of the proposed iterative algorithm depends on the initial values of the algorithm, we propose a simple method to provide initial values using three pilot signals. ...

Based on the closed simplified form of the optimal phase shifts for all phase-shifting elements of the LISBT, we have got the model as a function of sinc function. The sinc function has one central lobe and many side lobes. Based on the property of sinc function [7], we tried to explore the unimodality, lipschitz and concavity property of the estimated channel model. Some authors worked on unimodal bandits [10], lipschitz bandits [12] and Convex bandits [1]. The sinc function takes unimodal nature if we take some equidistant points within an interval such that there exist at most one point in each lobe. But as our focus is to reduce the number of pilot signals, hence estimating the parameters of optimal shifts exploiting unimodal nature of sinc functions will require large number of pilots. The concavity property of since function holds for each lobe but not over the lobes. The sinc function also does not satisfy the lipschitz property. Hence, we propose an efficient scheme to obtain the unknown parameters based on the far-field channel model of a LISBT-assisted wireless communication model and to provide theoretical guarantee of the proposed scheme with numerical validations.

1.2 Main Contributions

This paper proposes a channel based estimation scheme on the path parameters of the LISBT-assisted wireless communication system and then estimate those parameters with the lowest possible number of pilots. Unlike the existing works, the training overhead and the computational cost of the proposed scheme does not scale with the the number of antennas. Our main contributions are as follows:

- We present an iterative algorithm based on the proposed scheme to estimate the unknown parameters of LISBT-assisted wireless communication system in the presence of noise at the receiver.
- We provided the performance guarantee of the proposed algorithm.

- We validated the performance guarantee through numerical simulations and compared the proposed algorithm with the potential benchmarks present in the literature.

The remaining part of this paper is organized as follows. The system model and channel model are described in Chapter 2. We obtain the optimal phase shifts at the LISBT in Chapter 3. In Chapter 3, we also provide channel models that hold in the far-field. We propose our estimation scheme in the case with and without receiver noise in Chapter 4. The simulation results are provided in Chapter 5. Finally, Chapter 6 concludes the paper.

Chapter 2

System Model

In this section, we introduce the system and channel models as given in the paper [6].

2.1 System Model

We consider a LISBT-assisted wireless communication system, where an LISBT communicates with a user [6]. The LISBT considers only one RF signal generator, generated at the backside of the LIS, that passes the signal through the LIS where each phase-shifting element changes the phase of the passing RF signal and able to send a beamformed signal towards the user, cf. Fig. 2.1.

The system model comprises of a rectangular surface based LIS of size $L_x \times L_y$, where L_x and L_y are the width and the length of the surface, respectively. The LISBT comprises of a large number of sub-wavelength phase-shifting elements where each elements is of size $L_e \times L_e$ that can change the phase and amplitude of the signal. Let us assume that the LIS lies in the $x-y$ plane of a Cartesian coordinate system where the center of the surface is placed at the origin of the coordinate system, cf. Fig. 2.1. Let d_r be the distance between neighboring phase-shifting elements. The total number of phase-shifting elements of the LISBT is given by $M = M_x \times M_y$, where $M_x = \frac{L_x}{d_r}$ and $M_y = \frac{L_y}{d_r}$. Assuming M_x and M_y are odd numbers, the position of the $(m_x, m_y)^{th}$ phase-shifting element in Cartesian coordinate system is given as $(x, y) = (m_x d_r, m_y d_r)$ where $m_x = -\frac{M_x-1}{2}, \ldots, \frac{M_x-1}{2}$ and $m_y = -\frac{M_y-1}{2}, \ldots, \frac{M_y-1}{2}$.

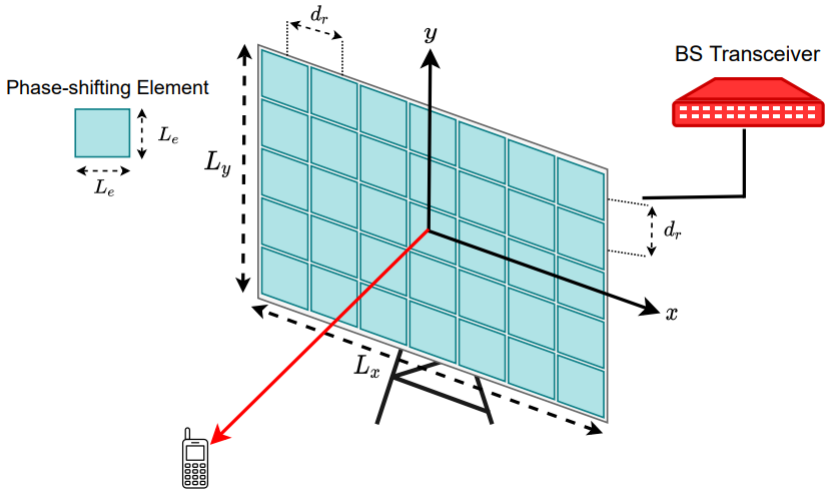

Figure 2.1: The LISBT-assisted wireless communication system where each phase-shifting element of the LIS changes the phase of the RF signal, and hence the LISBT is able to send a beamformed signal towards the user [6].

2.2 Channel Model

Generally, there are line-of-sight (LoS) and some non-line-of-sight (NLoS) components are present in the channel between two transceivers. We consider the LoS component to model the channel between the LISBT and the user as the power of LoS component is much higher than the power of Non-LoS component [2]. In the following, we model the channel between the LISBT and the user based on the path parameters of the system.

We will now model the LISBT-user channel between $(m_x, m_y)^{th}$ phase-shifting element at the LSBT and the user. Let $t_{m_x m_y}$ denote the channel coefficient between the $(m_x, m_y)^{th}$ phase-shifting element at the LISBT and the user. Due to the LoS assumption, $t_{m_x m_y}$ is given by

$$t_{m_x m_y} = \frac{\lambda \sqrt{F_{m_x m_y}}}{4\pi d_{m_x m_y}} e^{-jk_0 d_{m_x m_y}}, \forall m_x, m_y \tag{2.1}$$

where λ denotes the wavelength of the carrier frequency, $k_0 = \frac{2\pi}{\lambda}$ denotes the wave number, $d_{m_x m_y}$ denotes the distance between the center of the $(m_x, m_y)^{th}$ phase-shifting element at the LISBT and the user, and $F_{m_x m_y}$ denotes the effect of the size and power radiation pattern of the phase-shifting elements on the channel coefficient.

Since each phase-shifting element can be configured to impose different levels of phase shift on the transmitted and received signal [15], we denote $\Gamma_{m_x m_y} =$

$e^{j\beta_{m_x m_y}}$ as the beamforming weight of the $(m_x, m_y)^{th}$ phase-shifting element at the LISBT, where $\beta_{m_x m_y}$ is the phase shift at the $(m_x, m_y)^{th}$ element. Therefore, we define the phase shift parameters for all elements of the LISBT as $\beta = \{\beta_{m_x m_y}, \forall m_x, m_y\}$. Hence, the LISBT-user channel, denoted by $H(\beta)$, can be written as

$$\begin{aligned} H(\beta) &= \sum_{m_x=-\frac{M_x-1}{2}}^{\frac{M_x-1}{2}} \sum_{m_y=-\frac{M_y-1}{2}}^{\frac{M_y-1}{2}} \Gamma_{m_x m_y} t_{m_x m_y} \\ &= \frac{\lambda}{4\pi} \sum_{m_x=-\frac{M_x-1}{2}}^{\frac{M_x-1}{2}} \sum_{m_y=-\frac{M_y-1}{2}}^{\frac{M_y-1}{2}} \frac{\sqrt{F_{m_x m_y}}}{d_{m_x m_y}} e^{-j(k_0 d_{m_x m_y} - \beta_{m_x m_y})} \end{aligned} \tag{2.2}$$

Therefore, (2.2) gives a clear idea that the LISBT-user channel depends on the phase shift imposed by each elements at the LISBT and the distance of each element from the user.

Chapter 3

Optimal Phase-Shifts at the LISBT

In this section, we will optimise the phase shifts of each element such that the received power at the user is maximised and will find the exact expression of the optimal phase-shifts at the LISBT that maximises the received power at the user.

Based on (2.2), the received power at the user of LISBT-assisted wireless communication system, denoted by $P_r(\beta)$, is given as

$$\begin{aligned} P_r(\beta) &= P_t|H(\beta)|^2 \\ &= P_t\left(\frac{\lambda}{4\pi}\right)^2 \left| \sum_{m_x=-\frac{M_x-1}{2}}^{\frac{M_x-1}{2}} \sum_{m_y=-\frac{M_y-1}{2}}^{\frac{M_y-1}{2}} \frac{\sqrt{F_{m_x m_y}}}{d_{m_x m_y}} e^{-j(k_0 d_{m_x m_y} - \beta_{m_x m_y})} \right|^2 \end{aligned} \tag{3.1}$$

where P_t is the transmission power at the LISBT. The above (3.1) is maximised at

$$\beta_{m_x m_y} = mod(k_0 d_{m_x m_y}, 2\pi) \qquad \forall m_x, m_y \tag{3.2}$$

According to (3.2), we have to estimate $M = M_x \times M_y$ number of parameters which is equal to the total number of phase-shifting elements at the LISBT. In the following, we will show that the number of parameters that need to be estimated can be reduced significantly when we obtain a closed-form expression for $d_{m_x m_y}, \forall m_x, m_y$.

According to Fig. 3.1, θ and ϕ denote the elevation and azimuth angles of the signal from the user to the center of the LIS, d_0 denotes the distance between the user and the center of the LIS, $d_r\sqrt{m_x^2 + m_y^2}$ denotes the distance between the center of the LIS to the center of the $(m_x, m_y)^{th}$ phase-shifting element, δ_{m_x,m_y} denotes the angle between the vector from the center of the LIS to the user and the vector from the center of the LIS to the center of the $(m_x, m_y)^{th}$ phase-shifting element. By using the cosine rule we obtain $d_{m_x m_y}$ as a function of d_r, m_x, m_y, and

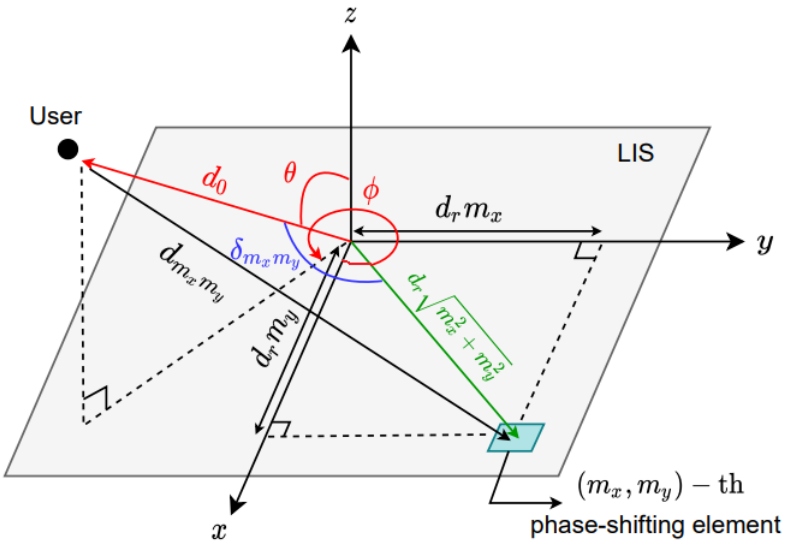

Figure 3.1: The cosin rule to obtain the distance between the $(m_x, m_y)^{th}$ phase-shifting element at the LISBT to the user.

$\delta_{m_x m_y}$ given by,

$$d_{m_x m_y} = \sqrt{d_0^2 + d_r^2(m_x^2 + m_y^2) - 2d_0 d_r \sqrt{m_x^2 + m_y^2} cos(\delta_{m_x m_y})} \tag{3.3}$$

Now, the vector from the user to the center of the LIS can be obtain as $[d_0 sin(\theta)cos(\phi), d_0 sin(\theta)sin(\phi), d_0 cos(\theta)]$, and the vector from the center of the LIS to the center of the $(m_x, my)^{th}$ phase-shifting element is $[d_r m_x, d_r m_y, 0]$. According to the inner product between these two vectors, we can write $cos(\delta_{m_x m_y})$ as,

$$\begin{aligned} cos(\delta_{m_x m_y}) &= \frac{[d_0 sin(\theta)cos(\phi), d_0 sin(\theta)sin(\phi), d_0 cos(\theta)].[d_r m_x, d_r m_y, 0]}{d_0 d_r \sqrt{m_x^2 + m_y^2}} \\ &= \frac{m_x sin(\theta)cos(\phi) + m_y sin(\theta)sin(\phi)}{\sqrt{m_x^2 + m_y^2}} \end{aligned} \tag{3.4}$$

Substituting (3.4) in (3.3), we obtain a much simpler expression for $d_{m_x m_y}$ as

$$d_{m_x m_y} = \sqrt{d_0^2 + d_r^2(m_x^2 + m_y^2) - 2d_0 d_r \sqrt{m_x \alpha_1 + m_y \alpha_2}} \tag{3.5}$$

$$\text{where, } \alpha_1 = sin(\theta)cos(\phi) \in [-1,1] \tag{3.6}$$

$$\alpha_2 = sin(\theta)sin(\phi) \in [-1,1] \tag{3.7}$$

By substitution (3.5) in (3.2) we get

$$\beta_{m_x m_y} = mod\left(k_0\left(d_0^2 + d_r^2(m_x^2+m_y^2) - 2d_0 d_r\sqrt{m_x\alpha_1 + m_y\alpha_2}\right)^{\frac{1}{2}}, 2\pi\right), \forall m_x, m_y. \tag{3.8}$$

According to the above (3.8), in order to obtain the optimal phase shift at the LISBT, instead of estimating M number of parameters we significantly reduced it to estimation of only three parameters d_0, α_1 and α_2. However, d_0 has to be estimated very precisely in order to set the optimal phase shifts, which is not possible in practice. Therefore, we will try to estimate only two parameters α_1 and α_2 overcoming the difficulty of estimation of d_0.

3.1 Far-Field Channel Model

In this section, we provide the LISBT-user channel models for the far-field regions. The far-field is referred to as the condition where the maximum phase error of the received signal on the antenna array does not exceed $\frac{\pi}{8}$ [14]. The distance between the user and the $(m_x, m_y)^{th}$ phase-shifting element at the LISBT in (3.5) can be rewritten as

$$d_{m_x m_y} = d_0\left(1 + \left(\frac{d_r^2(m_x^2+m_y^2)}{d_0^2} - \frac{2d_r(m_x\alpha_1 + m_y\alpha_2)}{d_0}\right)\right)^{\frac{1}{2}}$$

Following the same line of proof in [6], we use first-order Taylor's approximation, i.e $\sqrt{1+x} \approx 1 + \frac{x}{2}$ to get

$$d_{m_x m_y} = d_0 - d_r(m_x\alpha_1 + m_y\alpha_2) + \frac{d_r^2(m_x^2+m_y^2)}{2d_0} \tag{3.9}$$

Substituting (3.9) in (2.2), we get the LISBT-user channel for far-field region, denoted as $H^{(ff)}(\beta)$, given by

$$H^{(ff)}(\beta) \approx \frac{\lambda}{4\pi}\Bigg[\sum_{m_x=-\frac{M_x-1}{2}}^{\frac{M_x-1}{2}}\sum_{m_y=-\frac{M_y-1}{2}}^{\frac{M_y-1}{2}} \frac{\sqrt{F_{m_x m_y}}}{\left(d_0 - d_r(m_x\alpha_1 + m_y\alpha_2) + \frac{d_r^2(m_x^2+m_y^2)}{2d_0}\right)} e^{-j\left(k_0\left(d_0 - d_r(m_x\alpha_1+m_y\alpha_2) + \frac{d_r^2(m_x^2+m_y^2)}{2d_0}\right) - \beta_{m_x m_y}\right)}\Bigg] \tag{3.10}$$

When $\frac{d_r^2(m_x^2+m_y^2)}{2d_0}$ in the argument of the exponential term in (3.10) is much smaller than 2π, we can neglect its impact. Neglecting this term in (3.10) leads to the following maximum phase error

$$\max_{m_x,m_y} k_0 \left(\frac{d_r^2(m_x^2+m_y^2)}{2d_0} \right) = \frac{k_0 \left(\frac{L_x^2}{4} + \frac{L_y^2}{4} \right)}{2d_0} = \frac{k_0 D_{ITS}^2}{8d_0}, \tag{3.11}$$

where D_{ITS} is the diagonal of the LIS. Assuming a maximum phase error of $\frac{\pi}{8}$, the far-field region of the LISBT is obtained as

$$\frac{2\pi}{\lambda} \times \frac{D_{ITS}^2}{8d_0} \leq \frac{\pi}{8} \implies d_0 \geq \frac{2D_{ITS}^2}{\lambda}. \tag{3.12}$$

According to (3.12), as the size of the LIS is much smaller than d_0, we can approximate $\frac{1}{(d_0 - d_r(m_x\alpha_1 + m_y\alpha_2))} \approx \frac{1}{d_0}$. In addition, the radiation power pattern of all elements in the far-field region of the LISBT is the same, i.e., $F_{m_x m_y} = F$. Hence, by applying the above conditions and neglecting $\frac{d_r^2(m_x^2+m_y^2)}{2d_0}$ in the argument of the exponential term in (3.10), the LISBT-user channel in the far-field of the LISBT can be written as

$$H^{(ff)}(\beta) \approx \frac{\sqrt{F}\lambda e^{-jk_0 d_0}}{4\pi d_0} \sum_{m_x=-\frac{M_x-1}{2}}^{\frac{M_x-1}{2}} \sum_{m_y=-\frac{M_y-1}{2}}^{\frac{M_y-1}{2}} e^{j\left(k_0 d_r(m_x\alpha_1 + m_y\alpha_2) + \beta_{m_x m_y}\right)} \tag{3.13}$$

From (3.13), $H^{(ff)}(\beta)$ is maximised by

$$\beta_{m_x m_y} = -mod(k_0 d_r(m_x\alpha_1 + m_y\alpha_2), 2\pi), \forall m_x, m_y. \tag{3.14}$$

From (3.14), we can conclude that in order to obtain the optimal phase shift for maximizing the LISBT-user channel in the far-field region of the LISBT, we need to estimate only two parameters, α_1 and α_2. Since we do not have the values of α_1 and α_2, we consider a general case to see what would be the LISBT-user channel in the far-field of the LISBT if we replace α_1 and α_2 with any other values. In the following lemma, we apply a linear phase shift to each phase-shifting element to obtain a closed-form expression for the LISBT-user channel in the far-field of the LISBT. We consider the same line of proof of lemma as given in [6].

Lemma 1. *If we apply the following linear phase shift to the* $(m_x, m_y)^{th}$ *element*

$$\beta_{m_x m_y} = -mod(k_0 d_r(m_x\beta_1 + m_y\beta_2), 2\pi), \forall m_x, m_y, \tag{3.15}$$

then, the LISBT-user channel in the far-field of the LISBT is a function of β_1 and β_2, and can be obtained as

$$H^{(ff)}(\beta) \approx \left(\frac{\sqrt{F}\lambda e^{-jk_0d_0}}{4\pi d_0}\right)\left(\frac{sin\left(\frac{k_0L_x}{2}(\alpha_1-\beta_1)\right)}{sin\left(\frac{k_0d_r}{2}(\alpha_1-\beta_1)\right)}\right)\left(\frac{sin\left(\frac{k_0L_y}{2}(\alpha_2-\beta_2)\right)}{sin\left(\frac{k_0d_r}{2}(\alpha_2-\beta_2)\right)}\right) \tag{3.16}$$

Proof. By substituting (3.15) in (3.13), we get,

$$\begin{aligned} H^{(ff)}(\beta) &\approx \frac{\sqrt{F}\lambda e^{-jk_0d_0}}{4\pi d_0}\sum_{m_x=-\frac{M_x-1}{2}}^{\frac{M_x-1}{2}}\sum_{m_y=-\frac{M_y-1}{2}}^{\frac{M_y-1}{2}} e^{j\left(k_0d_r(m_x(\alpha_1-\beta_1)+m_y(\alpha_2-\beta_2))\right)} \\ &\approx \frac{\sqrt{F}\lambda e^{-jk_0d_0}}{4\pi d_0}\sum_{m_x=-\frac{M_x-1}{2}}^{\frac{M_x-1}{2}} e^{jk_0d_r(m_x(\alpha_1-\beta_1))}\sum_{m_y=-\frac{M_y-1}{2}}^{\frac{M_y-1}{2}} e^{jk_0d_r\left(m_y(\alpha_2-\beta_2)\right)} \end{aligned}$$

We can write the sum of terms in a geometric progression as $\sum_{m=-\frac{M-1}{2}}^{\frac{M-1}{2}} e^{jma} = \frac{e^{-j\left(\frac{M-1}{2}\right)a}\left(1-e^{jMa}\right)}{1-e^{ja}} = \frac{sin\left(\frac{Ma}{2}\right)}{sin\left(\frac{a}{2}\right)}$. Applying this in (3.17) and by substituting $M_x = L_x/d_r$ and $M_y = L_y/d_r$ we get,

$$\implies H^{(ff)}(\beta) \approx \left(\frac{\sqrt{F}\lambda e^{-jk_0d_0}}{4\pi d_0}\right)\left(\frac{sin\left(\frac{k_0L_x}{2}(\alpha_1-\beta_1)\right)}{sin\left(\frac{k_0d_r}{2}(\alpha_1-\beta_1)\right)}\right)\left(\frac{sin\left(\frac{k_0L_y}{2}(\alpha_2-\beta_2)\right)}{sin\left(\frac{k_0d_r}{2}(\alpha_2-\beta_2)\right)}\right)$$

■

For the extremely sub-wavelength elements ($d_r \to 0$), the LIS acts as a continuous surface [8]. Assuming $d_r \to 0$, we can approximate $sin\left(\frac{k_0d_r}{2}(\alpha_1-\beta_1)\right)$ and $sin\left(\frac{k_0d_r}{2}(\alpha_2-\beta_2)\right)$ with $\left(\frac{k_0d_r}{2}(\alpha_1-\beta_1)\right)$ and $\left(\frac{k_0d_r}{2}(\alpha_2-\beta_2)\right)$ respectively. Then, the LISBT-user channel in the far-field of the LISBT in (3.16) can be written as

$$H^{(ff)}(\beta) \approx \left(\frac{\sqrt{F}\lambda e^{-jk_0d_0}}{4\pi d_0}\right)M_x.M_y.sinc\left(\frac{k_0L_x}{2}(\alpha_1-\beta_1)\right)sinc\left(\frac{k_0L_y}{2}(\alpha_2-\beta_2)\right) \tag{3.17}$$

where $sinc(x) = \frac{sin(x)}{x}$. According to (3.17), the absolute value of the LISBT-user channel would be maximized when the sinc functions attain their maximum

value,i.e., when $\beta_1 = \alpha_1$ and $\beta_2 = \alpha_2$, respectively. Therefore, when we use the far-field channel model, we only need to estimate two parameters, α_1 and α_2. Compared with the optimal phase shift in (3.8), we observe that the number of parameters needed to be estimated decreases from three to two. Most importantly, we have avoided the estimation of d_0, which was the problematic parameter for estimation.

Chapter 4

Proposed Channel Estimation Strategy

In this section, we first propose the channel estimation scheme that estimates the optimal β_1 and β_2 that would maximize the received power at the user of the LISBT-assisted wireless communication system. We propose the estimation strategy for two scenarios. We first propose the channel estimation scheme under the assumption that there is no noise in the system. Then, we propose an iterative algorithm for the channel estimation scheme for the far-field scenario in the presence of the noise.

4.1 Channel Estimation in the Absence of Noise

In the channel estimation procedure, the user sends the pilot signal $x_p = \sqrt{P_p}$ to the LISBT, where P_p is the pilot transmit power. In the absence of the noise, the received signal at the LISBT is given by,

$$\begin{aligned} y(\beta_1,\beta_2) &= \sqrt{P_p} H^{(ff)}(\beta_1,\beta_2) \\ &= \sqrt{P_p}\left(\frac{\sqrt{F}\lambda e^{-jk_0d_0}}{4\pi d_0}\right) M_x.M_y.sinc\left(K_x(\alpha_1-\beta_1)\right) sinc\left(K_y(\alpha_2-\beta_2)\right) \end{aligned}$$

where $L_x = K_x\lambda$ and $L_y = K_y\lambda$, and $K_x, K_y \in \mathbb{N}$ are integers. The absolute the received signal at the LISBT is given by

$$|y(\beta_1,\beta_2)| = \left|\sqrt{P_p}\left(\frac{\sqrt{F}\lambda e^{-jk_0d_0}}{4\pi d_0}\right) M_x.M_y.sinc\left(K_x(\alpha_1-\beta_1)\right) sinc\left(K_y(\alpha_2-\beta_2)\right)\right| \tag{4.1}$$

The LISBT applies a new phase shift to the elements by changing β_1 and β_2, and before sending the first pilot, let the LSIBT sets $\beta_1 = \hat{\beta}_1$ and $\beta_2 = \hat{\beta}_2$, where $\hat{\beta}_1$ and $\hat{\beta}_2$ are two random numbers in the interval [-1,1]. Note that, according to (3.6) and (3.7), α_1 and α_2 are in the range of -1 to 1. Then, the absolute value of the received signal at the LISBT at $\hat{\beta}_1$ and $\hat{\beta}_2$ is given by,

$$\left|y(\hat{\beta}_1,\hat{\beta}_2)\right| = \left|\sqrt{P_p}\left(\frac{\sqrt{F}\lambda e^{-jk_0d_0}}{4\pi d_0}\right) M_x.M_y.sinc\left(K_x(\alpha_1-\hat{\beta}_1)\right) sinc\left(K_y(\alpha_2-\hat{\beta}_2)\right)\right| \tag{4.2}$$

Before sending the second pilot, let the LSIBT sets $\beta_1 = \hat{\beta}_1 + v$ and $\beta_2 = \hat{\beta}_2$, where v is any arbitrary parameter such that $K_x v \in \mathbb{N}$. Therefore, the absolute value of the received signal at the LISBT is given by

$$\left|y(\hat{\beta}_1+v,\hat{\beta}_2)\right| = \left|\sqrt{P_p}\left(\frac{\sqrt{F}\lambda e^{-jk_0d_0}}{4\pi d_0}\right) M_x.M_y.sinc\left(K_x(\alpha_1-\hat{\beta}_1-v)\right) sinc\left(K_y(\alpha_2-\hat{\beta}_2)\right)\right| \tag{4.3}$$

Dividing (4.2) by (4.3) we get

$$\begin{aligned}\frac{\left|y(\hat{\beta}_1,\hat{\beta}_2)\right|}{\left|y(\hat{\beta}_1+v,\hat{\beta}_2)\right|} &= \frac{\left|\sqrt{P_p}\left(\frac{\sqrt{F}\lambda e^{-jk_0d_0}}{4\pi d_0}\right) M_x.M_y.sinc\left(K_x(\alpha_1-\hat{\beta}_1)\right) sinc\left(K_y(\alpha_2-\hat{\beta}_2)\right)\right|}{\left|\sqrt{P_p}\left(\frac{\sqrt{F}\lambda e^{-jk_0d_0}}{4\pi d_0}\right) M_x.M_y.sinc\left(K_x(\alpha_1-\hat{\beta}_1-v)\right) sinc\left(K_y(\alpha_2-\hat{\beta}_2)\right)\right|} \\ &\approx \frac{\left|sinc\left(K_x(\alpha_1-\hat{\beta}_1)\right)\right|}{\left|sinc\left(K_x(\alpha_1-\hat{\beta}_1-v)\right)\right|}\end{aligned} \tag{4.4}$$

If v is selected such that $K_x v \in \mathbb{N}$, we have $sin(K_x\pi(\alpha_1-\hat{\beta}_1-v)) = sin(K_x\pi(\alpha_1-\hat{\beta}_1))$. Then, (4.4) can be simplified to

$$\frac{\left|y(\hat{\beta}_1,\hat{\beta}_2)\right|}{\left|y(\hat{\beta}_1+v,\hat{\beta}_2)\right|} \approx \left|\frac{\alpha_1-\hat{\beta}_1-v}{\alpha_1-\hat{\beta}_1}\right| \tag{4.5}$$

By solving the nonlinear equation (4.5), we get

$$\left|\frac{\alpha_1-\hat{\beta}_1-v}{\alpha_1-\hat{\beta}_1}\right| \approx \frac{\left|y(\hat{\beta}_1,\hat{\beta}_2)\right|}{\left|y(\hat{\beta}_1+v,\hat{\beta}_2)\right|}$$

$$\Rightarrow \frac{\alpha_1 - \hat{\beta}_1 - v}{\alpha_1 - \hat{\beta}_1} \approx \pm \frac{\left|y(\hat{\beta}_1, \hat{\beta}_2)\right|}{\left|y(\hat{\beta}_1 + v, \hat{\beta}_2)\right|}$$

$$\Rightarrow (\alpha_1 - \hat{\beta}_1 - v)\left|y(\hat{\beta}_1 + v, \hat{\beta}_2)\right| \approx (\alpha_1 - \hat{\beta}_1)\left(\pm\left|y(\hat{\beta}_1, \hat{\beta}_2)\right|\right)$$

$$\Rightarrow (\alpha_1 - \hat{\beta}_1)\left|y(\hat{\beta}_1 + v, \hat{\beta}_2)\right| - (\alpha_1 - \hat{\beta}_1)\left(\pm\left|y(\hat{\beta}_1, \hat{\beta}_2)\right|\right) \approx v\left|y(\hat{\beta}_1 + v, \hat{\beta}_2)\right|$$

$$\Rightarrow (\alpha_1 - \hat{\beta}_1)\left(\left|y(\hat{\beta}_1 + v, \hat{\beta}_2)\right| \pm \left|y(\hat{\beta}_1, \hat{\beta}_2)\right|\right) \approx v\left|y(\hat{\beta}_1 + v, \hat{\beta}_2)\right|$$

$$\Rightarrow \alpha_1 = \hat{\beta}_1 + \frac{\left|y(\hat{\beta}_1 + v, \hat{\beta}_2)\right|}{\left(\left|y(\hat{\beta}_1 + v, \hat{\beta}_2)\right| \pm \left|y(\hat{\beta}_1, \hat{\beta}_2)\right|\right)} v$$

By solving the above equations, two answers for α_1, denoted by $\alpha_1^{(1)}$ and $\alpha_1^{(2)}$, can be obtained as

$$\Rightarrow \alpha_1^{(1)}, \alpha_1^{(2)} = \hat{\beta}_1 + \frac{\left|y(\hat{\beta}_1 + v, \hat{\beta}_2)\right|}{\left(\left|y(\hat{\beta}_1 + v, \hat{\beta}_2)\right| \pm \left|y(\hat{\beta}_1, \hat{\beta}_2)\right|\right)} v \tag{4.6}$$

In order to identify the correct solution for α_1, the LISBT sets the third pilot signal $\beta_1 = \hat{\beta}_1 - v$ and $\beta_2 = \hat{\beta}_2$. Using the received signal of the first and third pilot signals, two other solutions for α_1, denoted by $\alpha_1^{(3)}$ and $\alpha_1^{(4)}$, can be similarly obtained as

$$\alpha_1^{(3)}, \alpha_1^{(4)} = \hat{\beta}_1 + \frac{\left|y(\hat{\beta}_1 - v, \hat{\beta}_2)\right|}{\left(-\left|y(\hat{\beta}_1 - v, \hat{\beta}_2)\right| \pm \left|y(\hat{\beta}_1, \hat{\beta}_2)\right|\right)} v \tag{4.7}$$

Finally, using (4.6) and (4.7), α_1 can be estimated as

$$\hat{\alpha}_1 = \left\{ \frac{\alpha_1^{(i)} + \alpha_1^{(j)}}{2} : \min_{i,j} \left|\alpha_1^{(i)} - \alpha_1^{(j)}\right|; i \in \{1,2\}, j \in \{3,4\} \right\}. \tag{4.8}$$

In order to obtain α_2, two more pilot signals are needed to be sent by the user. For these two pilot signals, the LISBT sets two different phase shifts as $(\beta_1, \beta_2) = \{(\hat{\beta}_1, \hat{\beta}_2), (\hat{\beta}_1, \hat{\beta}_2 + w), (\hat{\beta}_1, \hat{\beta}_2 - w)\}$, where w is selected such that $K_y w \in \mathbb{N}$. Then, similar to α_1, we have the following solutions for α_2 as

$$\alpha_2^{(1)}, \alpha_2^{(2)} = \hat{\beta}_2 + \frac{\left|y(\hat{\beta}_1, \hat{\beta}_2 + w)\right|}{\left(\left|y(\hat{\beta}_1, \hat{\beta}_2) + w\right| \pm \left|y(\hat{\beta}_1, \hat{\beta}_2)\right|\right)} w \tag{4.9}$$

$$\alpha_2^{(3)}, \alpha_2^{(4)} = \hat{\beta}_2 + \frac{\left|y(\hat{\beta}_1, \hat{\beta}_2 - w)\right|}{\left(-\left|y(\hat{\beta}_1, \hat{\beta}_2 - w)\right| \pm \left|y(\hat{\beta}_1, \hat{\beta}_2)\right|\right)} w \tag{4.10}$$

Finally, using (4.9) and (4.10), α_2 can be estimated as

$$\hat{\alpha}_2 = \left\{ \frac{\alpha_2^{(i)} + \alpha_2^{(j)}}{2} : \min_{i,j} \left|\alpha_2^{(i)} - \alpha_2^{(j)}\right|; i \in \{1,2\}, j \in \{3,4\} \right\}. \tag{4.11}$$

Therefore, we show that α_1 and α_2 can be estimated using five pilots sent by the user.

Remark 1: The random choices for $\hat{\beta}_1$ and $\hat{\beta}_2$ may leads to the null points of the sinc functions in (4.2), which occurs at $\hat{\beta}_1 = \alpha_1 \pm \frac{q}{K_x}$ and $\hat{\beta}_2 = \alpha_2 \pm \frac{q}{K_y}$, where $q \in \mathbb{N}$. For these unfortunate initial values, the received signals at the LISBT are zero, and hence we cannot estimate α_1 and α_2. Since the initial values are chosen randomly, the probability of occurrence at the null points of the sinc functions are close to zero. However, if this happens, we change the initial values from $\hat{\beta}_1$ and $\hat{\beta}_2$ to $\hat{\beta}_1 + \frac{1}{2K_x}$ and $\hat{\beta}_2 + \frac{1}{2K_y}$, respectively, to move from the nulls to their closest peaks.

4.2 Channel Estimation in the presence of Noise

In the presence of the noise, the received signal at the user is given by

$$y(\beta_1, \beta_2) = \sqrt{P_p} \times H^{(ff)}(\beta_1, \beta_2) + n \tag{4.12}$$

The received signal strength is defined as

$$r(\beta_1, \beta_2) = |y(\beta_1, \beta_2)| \tag{4.13}$$

where n denotes the additive white Gaussian noise (AWGN) with mean 0 and variance σ^2 at the LISBT, (β_1, β_2) are the parameters that specify the phase shift at the LIS. We assume that α_1, α_2 are unknown.

Objective: Identify $(\beta_1^*, \beta_2^*) = \arg\max_{\beta_1, \beta_2 \in \chi} r(\beta_1, \beta_2)$ where the search space $\chi = [-1, 1]$. Due to noisy, we consider the expected value of $r^2(\beta_1, \beta_2)$ and we denote the expected value as $\mu(\beta_1, \beta_2) = \mathbb{E}\left[r^2(\beta_1, \beta_2)\right] = \sigma^2 + \left|\sqrt{P_p} \times H^{(ff)}(\beta_1, \beta_2)\right|^2$. We assume that σ^2 is known. Hence, we would identify $(\beta_1^*, \beta_2^*) = \arg\max_{\beta_1, \beta_2 \in \chi} \mathbb{E}\left[r^2(\beta_1, \beta_2)\right]$ where the search space $\chi = [-1, 1]$.

4.2.1 Estimation α_1 and α_2 by $\mu(\beta_1,\beta_2)$

We will consider five pilot signals given as,

$$B=\left\{\left(\hat{\beta}_1,\hat{\beta}_2\right),\left(\hat{\beta}_1+v,\hat{\beta}_2\right),\left(\hat{\beta}_1-v,\hat{\beta}_2\right),\left(\hat{\beta}_1,\hat{\beta}_2+w\right),\left(\hat{\beta}_1,\hat{\beta}_2-w\right)\right\}.$$

$$\mu\left(\hat{\beta}_1,\hat{\beta}_2\right)=\sigma^2+\left|\sqrt{P_p}\left(\frac{\sqrt{F}\lambda e^{-jk_0d_0}}{4\pi d_0}\right)M_xM_y.sinc\left(K_x(\alpha_1-\hat{\beta}_1)\right)sinc\left(K_y(\alpha_2-\hat{\beta}_2)\right)\right|^2$$

$$\mu\left(\hat{\beta}_1+v,\hat{\beta}_2\right)=\sigma^2+\left|\sqrt{P_p}\left(\frac{\sqrt{F}\lambda e^{-jk_0d_0}}{4\pi d_0}\right)M_xM_y.sinc\left(K_x(\alpha_1-\hat{\beta}_1-v)\right)sinc\left(K_y(\alpha_2-\hat{\beta}_2)\right)\right|^2$$

$$\mu\left(\hat{\beta}_1-v,\hat{\beta}_2\right)=\sigma^2+\left|\sqrt{P_p}\left(\frac{\sqrt{F}\lambda e^{-jk_0d_0}}{4\pi d_0}\right)M_xM_y.sinc\left(K_x(\alpha_1-\hat{\beta}_1+v)\right)sinc\left(K_y(\alpha_2-\hat{\beta}_2)\right)\right|^2$$

$$\mu\left(\hat{\beta}_1,\hat{\beta}_2+w\right)=\sigma^2+\left|\sqrt{P_p}\left(\frac{\sqrt{F}\lambda e^{-jk_0d_0}}{4\pi d_0}\right)M_xM_y.sinc\left(K_x(\alpha_1-\hat{\beta}_1)\right)sinc\left(K_y(\alpha_2-\hat{\beta}_2-w)\right)\right|^2$$

$$\mu\left(\hat{\beta}_1,\hat{\beta}_2-w\right)=\sigma^2+\left|\sqrt{P_p}\left(\frac{\sqrt{F}\lambda e^{-jk_0d_0}}{4\pi d_0}\right)M_xM_y.sinc\left(K_x(\alpha_1-\hat{\beta}_1)\right)sinc\left(K_y(\alpha_2-\hat{\beta}_2+w)\right)\right|^2$$

Evaluating the above equations we get

$$\hat{\alpha_1}^{(1)/(2)}=\hat{\beta}_1+\frac{v}{1\pm\sqrt{\frac{\mu(\hat{\beta}_1,\hat{\beta}_2)-\sigma^2}{\mu(\hat{\beta}_1+v,\hat{\beta}_2)-\sigma^2}}}\text{ and }\hat{\alpha_1}^{(3)/(4)}=\hat{\beta}_1+\frac{v}{-1\pm\sqrt{\frac{\mu(\hat{\beta}_1,\hat{\beta}_2)-\sigma^2}{\mu(\hat{\beta}_1-v,\hat{\beta}_2)-\sigma^2}}}$$

where v is selected such that $K_xv\in\mathbb{N}$. We estimate α_1 as

$$\tilde{\alpha_1}=\left\{\frac{\hat{\alpha_1}^{(i)}+\hat{\alpha_1}^{(j)}}{2}:\min_{i,j}\left|\hat{\alpha_1}^{(i)}-\hat{\alpha_1}^{(j)}\right|;i\in\{1,2\},j\in\{3,4\}\right\}\tag{4.14}$$

$$\hat{\alpha_2}^{(1)/(2)}=\hat{\beta}_2+\frac{w}{1\pm\sqrt{\frac{\mu(\hat{\beta}_1,\hat{\beta}_2)-\sigma^2}{\mu(\hat{\beta}_1,\hat{\beta}_2+w)-\sigma^2}}}\text{ and }\hat{\alpha_2}^{(3)/(4)}=\hat{\beta}_2+\frac{w}{-1\pm\sqrt{\frac{\mu(\hat{\beta}_1,\hat{\beta}_2)-\sigma^2}{\mu(\hat{\beta}_1,\hat{\beta}_2-w)-\sigma^2}}}$$

where w is selected such that $K_yw\in\mathbb{N}$. We estimate α_2 as

$$\tilde{\alpha_2}=\left\{\frac{\hat{\alpha_2}^{(i)}+\hat{\alpha_2}^{(j)}}{2}:\min_{i,j}\left|\hat{\alpha_2}^{(i)}-\hat{\alpha_2}^{(j)}\right|;i\in\{1,2\},j\in\{3,4\}\right\}\tag{4.15}$$

Remark 2: The random choices for $\hat{\beta}_1$ and $\hat{\beta}_2$ may leads to the null points of the sinc functions in (4.2), which occurs at $\hat{\beta}_1=\alpha_1\pm\frac{q}{K_x}$ and $\hat{\beta}_2=\alpha_2\pm\frac{q}{K_y}$, where

$q \in \mathbb{N}$. For these unfortunate initial values, the received signals at the LISBT are zero, and hence we cannot estimate α_1 and α_2. Since the initial values are chosen randomly, the probability of occurrence at the null points of the sinc functions are close to zero. However, if this happens, we change the initial values from $\hat{\beta}_1$ and $\hat{\beta}_2$ to $\hat{\beta}_1 + \frac{1}{2K_x}$ and $\hat{\beta}_2 + \frac{1}{2K_y}$, respectively, to move from the nulls to their closest peaks.

4.2.2 Proposed Algorithm

We first provided a possible good choice of initial values of β_1 and β_2 and then proposed an algorithm of finding the optimal solution β_1 and β_2 that maximizes the expected square of received signal strength.

Initial values for the Proposed Algorithm

The performance of the proposed algorithm depends on the initial values of $(\hat{\beta}_1, \hat{\beta}_2)$. When the initial values of the proposed algorithm are random, it means that the LISBT focuses the pilot signals towards random directions. As a result, the received signal at the user may be comparable to the noise, which degrades the performance of the iterative algorithm. On the other hand, when the initial values are close to α_1 and α_2, the iterative algorithm can accurately estimate α_1 and α_2. In the following, we propose a simple method to provide the initial values of $(\hat{\beta}_1, \hat{\beta}_2)$ close to α_1 and α_2. We follow the draft [6] for the procedure. Our proposed algorithm is based on empirical means of the five points that are calculated over T number of time-slots.

We proposed an algorithm, c.f. Algorithm 1, that operates in two phases. In the first phase, we apply Uniform Exploration to obtain the empirical means of the five points in the first stage. This algorithm takes the minimum pilots to estimate the means of the arms. Based on the estimated means of each pilots, we propose the second phase of the algorithm where we define mathematical formulation in estimating α_1 and α_2 based on the estimated means.

Algorithm 1 Two-phase Phase Estimation Algorithm

Input: $B = \left\{ \left(\hat{\beta}_1, \hat{\beta}_2\right), \left(\hat{\beta}_1 + v, \hat{\beta}_2\right), \left(\hat{\beta}_1 - v, \hat{\beta}_2\right), \left(\hat{\beta}_1, \hat{\beta}_2 + w\right), \left(\hat{\beta}_1, \hat{\beta}_2 - w\right) \right\}$

Input: T

Phase 1: Uniform Exploration Algorithm

Initialize: $K = |B|$
for $t = 1$ to K **do**
  Sample arm k a total of $\lfloor T/K \rfloor$ times.
  Compute $\hat{\mu}_k$ the sample mean of arm k.
end for
Output: $\hat{\mu}_k, k \in [K]$.

Phase 2: Estimate α_1 and α_2

Input: σ^2.
Input: Apply Phase 1 of Algorithm 1 to get $\hat{\mu}_k, k \in [K]$.

Obtain $\tilde{\alpha}_1$ as given by $\tilde{\alpha_1} = \left\{ \frac{\hat{\alpha_1}^{(i)} + \hat{\alpha_1}^{(j)}}{2} : \min_{i,j} \left| \hat{\alpha_1}^{(i)} - \hat{\alpha_1}^{(j)} \right| ; i \in \{1,2\}, j \in \{3,4\} \right\}$

where $\hat{\alpha_1}^{(1)/(2)} = \hat{\beta}_1 + \frac{v}{1 \pm \sqrt{\left| \frac{\hat{\mu}(\hat{\beta}_1, \hat{\beta}_2) - \sigma^2}{\hat{\mu}(\hat{\beta}_1 + v, \hat{\beta}_2) - \sigma^2} \right|}}$

and $\hat{\alpha_1}^{(3)/(4)} = \hat{\beta}_1 + \frac{v}{-1 \pm \sqrt{\left| \frac{\hat{\mu}(\hat{\beta}_1, \hat{\beta}_2) - \sigma^2}{\hat{\mu}(\hat{\beta}_1 - v, \hat{\beta}_2) - \sigma^2} \right|}}$

Obtain $\tilde{\alpha}_2$ as given by $\tilde{\alpha_2} = \left\{ \frac{\hat{\alpha_2}^{(i)} + \hat{\alpha_2}^{(j)}}{2} : \min_{i,j} \left| \hat{\alpha_2}^{(i)} - \hat{\alpha_2}^{(j)} \right| ; i \in \{1,2\}, j \in \{3,4\} \right\}$

where $\hat{\alpha_2}^{(1)/(2)} = \hat{\beta}_2 + \frac{w}{1 \pm \sqrt{\left| \frac{\hat{\mu}(\hat{\beta}_1, \hat{\beta}_2) - \sigma^2}{\hat{\mu}(\hat{\beta}_1, \hat{\beta}_2 + w) - \sigma^2} \right|}}$

and $\hat{\alpha_2}^{(3)/(4)} = \hat{\beta}_2 + \frac{w}{-1 \pm \sqrt{\left| \frac{\hat{\mu}(\hat{\beta}_1, \hat{\beta}_2) - \sigma^2}{\hat{\mu}(\hat{\beta}_1, \hat{\beta}_2 - w) - \sigma^2} \right|}}$

Output: $\tilde{\alpha}_1$ and $\tilde{\alpha}_2$.

Chapter 5

Analysis of the Proposed Algorithm

In the presence of the noise, the received signal at the user is given by (4.1) and the received signal strength is given by

$$r(\beta_1,\beta_2) = |y(\beta_1,\beta_2)| = |G(\beta_1,\beta_2)+n|$$

where $G(\beta_1,\beta_2) = \sqrt{P_p}H^{(ff)}(\beta_1,\beta_2)$.

5.1 Distribution and mean of $\mathbf{r^2}(\beta_1,\beta_2)$

We know $n \sim CN(0,\sigma^2) \implies n = n_1 + jn_2,$ where n_1, n_2 are independent $\sim N\left(0,\frac{\sigma^2}{2}\right)$

$G(\beta_1,\beta_2) \in$ Complex number $\implies G(\beta_1,\beta_2) = a + jb$

Therefore, $y(\beta_1,\beta_2) = (a+n_1) + j(b+n_2)$

and $r^2(\beta_1,\beta_2) = (a+n_1)^2 + (b+n_2)^2$ (5.1)

As $a+n_1 \sim N\left(a,\frac{\sigma^2}{2}\right)$ and $b+n_2 \sim N\left(b,\frac{\sigma^2}{2}\right)$ are independent

$\left(\frac{a+n_1}{\sigma/\sqrt{2}}\right)^2 \sim \chi_1^2\left(\left(\frac{a}{\sigma/\sqrt{2}}\right)^2\right)$ and $\left(\frac{b+n_2}{\sigma/\sqrt{2}}\right)^2 \sim \chi_1^2\left(\left(\frac{b}{\sigma/\sqrt{2}}\right)^2\right)$ are independent

Therefore, $\frac{2}{\sigma^2}r^2(\beta_1,\beta_2) \sim \chi_2^2\left(\frac{2}{\sigma^2}|G(\beta_1,\beta_2)|^2\right)$ (5.2)

and $\mathbb{E}\left[r^2(\beta_1,\beta_2)\right] = \mathbb{E}\left[\frac{\sigma^2}{2}\left(\frac{2}{\sigma^2}r^2(\beta_1,\beta_2)\right)\right] = \sigma^2 + |G(\beta_1,\beta_2)|^2$

(5.3)

Based on the above distribution and expectation, we get

$$\hat{\mu}(\beta_1,\beta_2) = \frac{1}{n}\sum_{t=1}^{n} r_t^2(\beta_1,\beta_2) = \frac{\sigma^2}{2n}\sum_{t=1}^{n}\frac{2}{\sigma^2} r_t^2(\beta_1,\beta_2)$$

$$\implies \hat{\mu}(\beta_1,\beta_2) = \frac{\sigma^2}{2n}X, \text{ where } X \sim \chi^2_{2n}(\lambda_x), \lambda_x = n\lambda_1, \text{ and } \lambda_1 = \frac{2}{\sigma^2}|G(\beta_1,\beta_2)|^2$$

Similarly, $\hat{\mu}(\beta_1+v,\beta_2) = \frac{\sigma^2}{2n}Y$, where $Y \sim \chi^2_{2n}(\lambda_y), \lambda_y = n\lambda_2$, and $\lambda_2 = \frac{2}{\sigma^2}|G(\beta_1+v,\beta_2)|^2$

and $\hat{\mu}(\beta_1-v,\beta_2) = \frac{\sigma^2}{2n}Z$, where $Z \sim \chi^2_{2n}(\lambda_z), \lambda_z = n\lambda_3$, and $\lambda_3 = \frac{2}{\sigma^2}|G(\beta_1-v,\beta_2)|^2$

Again, $\hat{\mu}(\beta_1,\beta_2+w) = \frac{\sigma^2}{2n}U$, where $U \sim \chi^2_{2n}(\lambda_u), \lambda_u = n\lambda_4$, and $\lambda_4 = \frac{2}{\sigma^2}|G(\beta_1,\beta_2+w)|^2$

and $\hat{\mu}(\beta_1,\beta_2-w) = \frac{\sigma^2}{2n}V$, where $V \sim \chi^2_{2n}(\lambda_v), \lambda_v = n\lambda_5$, and $\lambda_5 = \frac{2}{\sigma^2}|G(\beta_1,\beta_2-w)|^2$

where the random variables X, Y, Z, U and V are independent and v and w are selected such that $K_x v \in \mathbb{N}$ and $K_y w \in \mathbb{N}$, respectively.

5.2 Estimates of α_1 and α_2

We will first provide probabilistic bound of estimate of α_1. The approach of α_2 will follow the same line of proof.

We have five points defined as

$$B = \left\{ \left(\hat{\beta}_1,\hat{\beta}_2\right), \left(\hat{\beta}_1+v,\hat{\beta}_2\right), \left(\hat{\beta}_1-v,\hat{\beta}_2\right), \left(\hat{\beta}_1,\hat{\beta}_2+w\right), \left(\hat{\beta}_1,\hat{\beta}_2-w\right) \right\}.$$

According to the proposed algorithm, the estimate of α_1, denoted as $\tilde{\alpha}_1$, is given by

$$\tilde{\alpha}_1 = \left\{ \frac{\hat{\alpha_1}^{(i)} + \hat{\alpha_1}^{(j)}}{2} : \min_{i,j} \left| \hat{\alpha_1}^{(i)} - \hat{\alpha_1}^{(j)} \right|; i \in \{1,2\}, j \in \{3,4\} \right\}$$

$$\text{where } \hat{\alpha_1}^{(1)/(2)} = \hat{\beta}_1 + \frac{v}{1 \pm \sqrt{\left| \frac{\hat{\mu}(\hat{\beta}_1,\hat{\beta}_2) - \sigma^2}{\hat{\mu}(\hat{\beta}_1+v,\hat{\beta}_2) - \sigma^2} \right|}} = \hat{\beta}_1 + \frac{v}{1 \pm \sqrt{\left|\frac{X-2n}{Y-2n}\right|}} \tag{5.4}$$

$$\text{and } \hat{\alpha_1}^{(3)/(4)} = \hat{\beta}_1 + \frac{v}{-1 \pm \sqrt{\left| \frac{\hat{\mu}(\hat{\beta}_1,\hat{\beta}_2) - \sigma^2}{\hat{\mu}(\hat{\beta}_1-v,\hat{\beta}_2) - \sigma^2} \right|}} = \hat{\beta}_1 + \frac{v}{-1 \pm \sqrt{\left|\frac{X-2n}{Z-2n}\right|}} \tag{5.5}$$

Similarly, the estimate of α_2, denoted as $\tilde{\alpha_2}$, is given by

$$\tilde{\alpha_2} = \left\{ \frac{\hat{\alpha_2}^{(i)} + \hat{\alpha_2}^{(j)}}{2} : \min_{i,j} \left| \hat{\alpha_2}^{(i)} - \hat{\alpha_2}^{(j)} \right| ; i \in \{1,2\}, j \in \{3,4\} \right\}$$

$$\text{where } \hat{\alpha_2}^{(1)/(2)} = \hat{\beta}_2 + \frac{v}{1 \pm \sqrt{\left| \frac{\hat{\mu}(\hat{\beta}_1, \hat{\beta}_2) - \sigma^2}{\hat{\mu}(\hat{\beta}_1, \hat{\beta}_2 + w) - \sigma^2} \right|}} = \hat{\beta}_1 + \frac{v}{1 \pm \sqrt{\left| \frac{X-2n}{U-2n} \right|}} \tag{5.6}$$

$$\text{and } \hat{\alpha_2}^{(3)/(4)} = \hat{\beta}_2 + \frac{v}{-1 \pm \sqrt{\left| \frac{\hat{\mu}(\hat{\beta}_1, \hat{\beta}_2) - \sigma^2}{\hat{\mu}(\hat{\beta}_1, \hat{\beta}_2 - w) - \sigma^2} \right|}} = \hat{\beta}_1 + \frac{v}{-1 \pm \sqrt{\left| \frac{X-2n}{V-2n} \right|}} \tag{5.7}$$

We will now discuss about the Sub-exponential distributions and its tail bound.

5.2.1 Sub-Exponential and its bounds

Definition: A random variable X with mean μ is said to be sub-exponential (ν, α) if $\mathbb{E}[exp\{t(X-\mu)\}] \leq exp\left(\frac{t^2\nu^2}{2}\right)$ whenever $|t| < \frac{1}{\alpha}$.

Example: If $X \sim \chi^2_p$, then X is sub-exponential $(2p, 4)$.

The following following proposition and lemma are followed from [16].

Proposition 1. *(Sub-exponential tail bound). Suppose that X is sub-exponential with parameters* (ν, b). *Then*

$$\mathbb{P}\{X \geq \mu + t\} \leq \begin{cases} e^{-\frac{t^2}{2\nu^2}}, & if\, 0 \leq t \leq \frac{\nu^2}{b}, \\ e^{-\frac{t}{2b}}, & if\, t \geq \frac{\nu^2}{b}. \end{cases}$$

As with the Hoeffding inequality, similar bounds apply to the left-sided event $X \leq \mu - t$, *as well as the two-sided event* $|X - \mu| \geq t$, *with an additional factor of two in the latter case.*

Theorem 2. *Suppose that* $X_k, k = 1, 2, \ldots, n$ *are independent, and that variable* X_k *is sub-exponential with parameters* (ν_k, b_k), *and has mean* $\mu_k = \mathbb{E}[X_k]$. *We compute the moment generating function as,*

$$\mathbb{E}\left[e^{t \sum_{k=1}^{n} (X_k - \mu_k)} \right] = \prod_{k=1}^{n} \mathbb{E}\left[e^{t(X_k - \mu_k)} \right] \qquad \textit{By independence of } X_k's$$

$$\leq \prod_{k=1}^{n} e^{\frac{\nu_k^2 t^2}{2}}, \quad \forall |t| < \left(\frac{1}{\max\limits_{k=1,2,\ldots,n} b_k} \right) \textit{ as } X_k \sim Subexp(\nu_k, b_k)$$

Therefore, $\sum_{k=1}^{n}(X_k-\mu_k) \sim Subexp(\nu_*, b_*)$, *where* $b_* = \max_{k=1,2\ldots,n} b_k$ *and* $\nu_* = \sqrt{\frac{\sum_{k=1}^{n}\nu_k^2}{n}}$.

By Proposition 1, the upper tail bound is given as

$$\mathbb{P}\left\{\left|\frac{1}{n}\sum_{k=1}^{n}(X_k-\mu_k)\right| \geq t\right\} \leq \begin{cases} 2.e^{-\frac{nt^2}{2\nu_*^2}}, & for\ 0 \leq t \leq \frac{\nu_*^2}{b_*} \\ 2.e^{-\frac{nt}{2b_*}}, & for\ t \geq \frac{\nu_*^2}{b_*} \end{cases}$$

Sub-exponential tail bound for Non-central Chi distribution:

In our case we have $X \sim \chi_p^2(a)$ with $\mathbb{E}[X] = p+a$.

$$\begin{aligned} \mathbb{E}[exp\{t(X-(p+a)\}] &= e^{-(p+a)t}\mathbb{E}[exp\{tX\}] \\ &= exp\left[\frac{2\lambda t^2}{1-2t} - \frac{p}{2}(\log(1-2t)+2t)\right] \\ &\leq e^{(\frac{[2(p+2a)]^2t^2}{2}}, \quad \forall |t| \leq 1/4 \\ \implies X &\sim \text{Sub-exponential}(2(p+2a),4). \end{aligned}$$

Corollary 1. *Let* $X_k, k = 1,2\ldots,n$ *are iid random variables from Sub-exponential with parameters* $(2(2+2a),4)$ *and has mean* $\mu_k = 2+a$. *Therefore,*

$$\mathbb{P}\left\{\left|\frac{1}{n}\sum_{k=1}^{n}(X_k-\mu_k)\right| \geq t\right\} \leq \begin{cases} 2.e^{-\frac{nt^2}{8(2+2a)^2}}, & for\ 0 \leq t \leq (2+2a)^2 \\ 2.e^{-\frac{nt}{8}}, & for\ t \geq (2+2a)^2 \end{cases}$$

5.2.2 Probabilistic Bound of $\tilde{\alpha}_1$

Proposition 3. *Let us denote events:*

$$A_{n,m} = \{|X_n - X_m| > \varepsilon\}, \quad A_n = \{|X_n - X| > \frac{\varepsilon}{2}\}, \quad A_m = \{|X_m - X| > \frac{\varepsilon}{2}\}$$

We need to show that $\mathbb{P}\{A_{n,m}\} \leq \mathbb{P}\{A_n\} + \mathbb{P}\{A_m\}$.

Proof. Let us define some events as,

$$A_{n,m} = \{|X_n - X_m| > \varepsilon\} = \{|X_n - X + X - X_m| > \varepsilon\}$$

$$
\begin{aligned}
&A_n = \{|X_n - X| > \frac{\varepsilon}{2}\} \\
&A_m = \{|X_m - X| > \frac{\varepsilon}{2}\} \\
&\mathbb{P}\{A_{n,m}\} = \mathbb{P}\{|X_n - X_m| > \varepsilon\} \\
&= \mathbb{P}\{|X_n - X + X - X_m| > \varepsilon\} \\
&\leq \mathbb{P}\{|X_n - X| + |X - X_m| > \varepsilon\} \\
&\text{since } A_{n,m} \subset \{|X_n - X| + |X - X_m| > \varepsilon\} \subset \left\{|X_n - X| > \frac{\varepsilon}{2} \bigcup |X - X_m| > \frac{\varepsilon}{2}\right\} \\
&\implies \mathbb{P}\{|X_n - X_m| > \varepsilon\} \leq \mathbb{P}\left\{|X_n - X| > \frac{\varepsilon}{2} \bigcup |X - X_m| > \frac{\varepsilon}{2}\right\} \\
&\leq \mathbb{P}\left\{|X_n - X| > \frac{\varepsilon}{2}\right\} + \mathbb{P}\left\{|X_m - X| > \frac{\varepsilon}{2}\right\} \\
&\implies \mathbb{P}\{A_{n,m}\} \leq \mathbb{P}\{A_n\} + \mathbb{P}\{A_m\}
\end{aligned}
$$

■

We will now try to give an upper bound of $\mathbb{P}\{|\tilde{\alpha}_1 - \alpha_1| \geq \varepsilon\}$.

Proof.

$$
\begin{aligned}
&\mathbb{P}\{|\tilde{\alpha}_1 - \alpha_1| \geq \varepsilon\} \\
&\quad \leq \mathbb{P}\left\{\left|\frac{\hat{\alpha_1}^{(1)} + \hat{\alpha_1}^{(3)}}{2} - \alpha_1\right| \geq \varepsilon\right\} + \mathbb{P}\left\{\left|\frac{\hat{\alpha_1}^{(1)} + \hat{\alpha_1}^{(4)}}{2} - \alpha_1\right| \geq \varepsilon\right\} \\
&\qquad\quad + \mathbb{P}\left\{\left|\frac{\hat{\alpha_1}^{(2)} + \hat{\alpha_1}^{(3)}}{2} - \alpha_1\right| \geq \varepsilon\right\} + \mathbb{P}\left\{\left|\frac{\hat{\alpha_1}^{(2)} + \hat{\alpha_1}^{(4)}}{2} - \alpha_1\right| \geq \varepsilon\right\} \\
&\quad = \text{(I)} + \text{(II)} + \text{(III)} + \text{(IV)} \qquad (5.8)
\end{aligned}
$$

By Proposition 3 we get

$$
\begin{aligned}
\text{(I)} \quad &\implies \leq \mathbb{P}\left\{\left|\hat{\alpha_1}^{(1)} - \alpha_1\right| \geq \varepsilon\right\} + \mathbb{P}\left\{\left|\hat{\alpha_1}^{(3)} - \alpha_1\right| \geq \varepsilon\right\} && (5.9) \\
\text{(II)} \quad &\implies \leq \mathbb{P}\left\{\left|\hat{\alpha_1}^{(1)} - \alpha_1\right| \geq \varepsilon\right\} + \mathbb{P}\left\{\left|\hat{\alpha_1}^{(4)} - \alpha_1\right| \geq \varepsilon\right\} && (5.10) \\
\text{(III)} \quad &\implies \leq \mathbb{P}\left\{\left|\hat{\alpha_1}^{(2)} - \alpha_1\right| \geq \varepsilon\right\} + \mathbb{P}\left\{\left|\hat{\alpha_1}^{(3)} - \alpha_1\right| \geq \varepsilon\right\} && (5.11) \\
\text{(IV)} \quad &\implies \leq \mathbb{P}\left\{\left|\hat{\alpha_1}^{(2)} - \alpha_1\right| \geq \varepsilon\right\} + \mathbb{P}\left\{\left|\hat{\alpha_1}^{(4)} - \alpha_1\right| \geq \varepsilon\right\} && (5.12)
\end{aligned}
$$

By eq. (5.8) we get

$$
\text{Hence, } \mathbb{P}\{|\tilde{\alpha}_1 - \alpha_1| \geq \varepsilon\} \leq 2\left(\mathbb{P}\left\{\left|\hat{\alpha_1}^{(1)} - \alpha_1\right| \geq \varepsilon\right\} + \mathbb{P}\left\{\left|\hat{\alpha_1}^{(2)} - \alpha_1\right| \geq \varepsilon\right\}\right.
$$

$$+\mathbb{P}\left\{\left|\hat{\alpha_1}^{(3)}-\alpha_1\right|\geq\varepsilon\right\}+\mathbb{P}\left\{\left|\hat{\alpha_1}^{(4)}-\alpha_1\right|\geq\varepsilon\right\}\Bigg) \tag{5.13}$$

Now we will try to bound each case.

$$\mathbb{P}\left\{\left|\hat{\alpha_1}^{(1)}-\alpha_1)\right|\geq\varepsilon\right\}=\mathbb{P}\left\{\left|\frac{v}{1+\sqrt{\left|\frac{X-2n}{Y-2n}\right|}}-(\alpha_1-\hat{\beta}_1)\right|\geq\varepsilon\right\}\quad\text{By eq. (5.4)}$$

We know $|X-Y|\leq|X|+|Y|$. Therefore, $\{|X-Y|\geq\varepsilon\}\implies\{|X|+|Y|\geq\varepsilon\}$. Applying this we get

$$\implies\mathbb{P}\left\{\left|\hat{\alpha_1}^{(1)}-\alpha_1)\right|\geq\varepsilon\right\}\leq\mathbb{P}\left\{\left|\frac{1}{1+\sqrt{\left|\frac{X-2n}{Y-2n}\right|}}\right|\geq\frac{1}{v}\left(\varepsilon-\left|\alpha_1-\hat{\beta}_1\right|\right)\right\}$$

Let us set $a=\frac{1}{v}\left(\varepsilon-\left|\alpha_1-\hat{\beta}_1\right|\right)$.

$$\mathbb{P}\left\{\left|\hat{\alpha_1}^{(1)}-\alpha_1)\right|\geq\varepsilon\right\}\leq\mathbb{P}\left\{\left|\frac{1}{1+\sqrt{\left|\frac{X-2n}{Y-2n}\right|}}\right|\geq a\right\}$$

Since $\frac{1}{1+\sqrt{\left|\frac{X-2n}{Y-2n}\right|}}\geq 0\implies\left|\frac{1}{1+\sqrt{\left|\frac{X-2n}{Y-2n}\right|}}\right|=\frac{1}{1+\sqrt{\left|\frac{X-2n}{Y-2n}\right|}}$, so we get

$$\mathbb{P}\left\{\left|\hat{\alpha_1}^{(1)}-\alpha_1)\right|\geq\varepsilon\right\}\leq\mathbb{P}\left\{\sqrt{\left|\frac{X-2n}{Y-2n}\right|}\leq\frac{1-a}{a}\right\}=\mathbb{P}\left\{\left|\frac{X-2n}{Y-2n}\right|\leq\left(1-\frac{1}{a}\right)^2\right\} \tag{5.14}$$

$$\begin{aligned}\mathbb{P}\left\{\left|\hat{\alpha_1}^{(2)}-\alpha_1)\right|\geq\varepsilon\right\}&=\mathbb{P}\left\{\left|\frac{v}{1-\sqrt{\left|\frac{X-2n}{Y-2n}\right|}}-(\alpha_1-\hat{\beta}_1)\right|\geq\varepsilon\right\}\qquad\text{By eq. (5.4)}\\&\leq\mathbb{P}\left\{\left|\frac{1}{1-\sqrt{\left|\frac{X-2n}{Y-2n}\right|}}\right|\geq\frac{1}{v}\left(\varepsilon-\left|\alpha_1-\hat{\beta}_1\right|\right)\right\}=\mathbb{P}\left\{\left|\frac{1}{1-\sqrt{\left|\frac{X-2n}{Y-2n}\right|}}\right|\geq a\right\}\\&=\mathbb{P}\left\{\left|1-\sqrt{\left|\frac{X-2n}{Y-2n}\right|}\right|\leq\frac{1}{a}\right\}=\mathbb{P}\left\{-\frac{1}{a}\leq 1-\sqrt{\left|\frac{X-2n}{Y-2n}\right|}\leq\frac{1}{a}\right\}\\&=\mathbb{P}\left\{\left(1-\frac{1}{a}\right)^2\leq\left|\frac{X-2n}{Y-2n}\right|\leq\left(\frac{1}{a}+1\right)^2\right\}\end{aligned}$$

$$\implies \mathbb{P}\left\{\left|\hat{\alpha_1}^{(2)} - \alpha_1)\right| \geq \varepsilon\right\} \leq \mathbb{P}\left\{\left|\frac{X-2n}{Y-2n}\right| \leq \left(1+\frac{1}{a}\right)^2\right\} - \mathbb{P}\left\{\left|\frac{X-2n}{Y-2n}\right| \leq \left(1-\frac{1}{a}\right)^2\right\} \tag{5.15}$$

By adding (5.14) and (5.15) we get

$$\mathbb{P}\left\{\left|\hat{\alpha_1}^{(1)} - \alpha_1)\right| \geq \varepsilon\right\} + \mathbb{P}\left\{\left|\hat{\alpha_1}^{(2)} - \alpha_1)\right| \geq \varepsilon\right\} \leq \mathbb{P}\left\{\left|\frac{Y-2n}{X-2n}\right| \geq \delta\right\}, \text{ where } \delta = \left(\frac{1}{1+(1/a)}\right)^2 \tag{5.16}$$

Similarly $\mathbb{P}\left\{\left|\hat{\alpha_1}^{(3)} - \alpha_1)\right| \geq \varepsilon\right\} + \mathbb{P}\left\{\left|\hat{\alpha_1}^{(4)} - \alpha_1)\right| \geq \varepsilon\right\} \leq \mathbb{P}\left\{\left|\frac{Z-2n}{X-2n}\right| \geq \delta\right\},$

Therefore, $\left(\mathbb{P}\left\{\left|\hat{\alpha_1}^{(1)} - \alpha_1)\right| \geq \varepsilon\right\} + \mathbb{P}\left\{\left|\hat{\alpha_1}^{(2)} - \alpha_1)\right| \geq \varepsilon\right\} + \mathbb{P}\left\{\left|\hat{\alpha_1}^{(3)} - \alpha_1)\right| \geq \varepsilon\right\}\right.$

$\left. + \mathbb{P}\left\{\left|\hat{\alpha_1}^{(4)} - \alpha_1)\right| \geq \varepsilon\right\}\right) \leq \mathbb{P}\left\{\left|\frac{Y-2n}{X-2n}\right| \geq \delta\right\} + \mathbb{P}\left\{\left|\frac{Z-2n}{X-2n}\right| \geq \delta\right\},$ (5.17)

Therefore, by eq. (5.13) we get

$$\mathbb{P}\{|\tilde{\alpha}_1 - \alpha_1| \geq \varepsilon\} \leq 2\left(\mathbb{P}\left\{\left|\frac{Y-2n}{X-2n}\right| \geq \delta\right\} + \mathbb{P}\left\{\left|\frac{Z-2n}{X-2n}\right| \geq \delta\right\}\right) \text{ where } \delta = \left(\frac{1}{1+(1/a)}\right)^2. \tag{5.18}$$

We have,

$$X_i \sim \chi^2_2(\lambda_1) \implies X_i \sim \text{Subexp}(2(2+\lambda_1),4) \text{ and } X = \sum_{i=1}^{n} X_i \sim \chi^2_{2n}(\lambda_x),$$

$$\text{where } \lambda_x = n\lambda_1, \text{ and } \lambda_1 = \frac{2}{\sigma^2}|G(\beta_1,\beta_2)|^2$$

$$Y_i \sim \chi^2_2(\lambda_2) \implies Y_i \sim \text{Subexp}(2(2+\lambda_2),4) \text{ and } Y = \sum_{i=1}^{n} Y_i \sim \chi^2_{2n}(\lambda_y),$$

$$\text{where } \lambda_y = n\lambda_2, \text{ and } \lambda_2 = \frac{2}{\sigma^2}|G(\beta_1+v,\beta_2)|^2,$$

$$Z_i \sim \chi^2_2(\lambda_3) \implies Z_i \sim \text{Subexp}(2(2+\lambda_3),4) \text{ and } Z = \sum_{i=1}^{n} Z_i \sim \chi^2_{2n}(\lambda_z),$$

$$\text{where } \lambda_z = n\lambda_3, \text{ and } \lambda_3 = \frac{2}{\sigma^2}|G(\beta_1-v,\beta_2)|^2,$$

Case 1: $\mathbb{P}\left\{\left|\frac{Y-2n}{X-2n}\right| \geq \delta\right\}$, where $\delta = \left(\frac{1}{1+\frac{v}{\varepsilon-\left|\alpha_1-\hat{\beta}_1\right|}}\right)^2$.

We know, $|Y-2n| = |Y-2n-n\lambda_2+n\lambda_2| \leq |Y-n(2+\lambda_2)|+n|\lambda_2|$ (5.19)

$$\mathbb{P}\{|Y-2n| \geq \delta|X-2n|\} \leq \int_0^\infty \mathbb{P}\{|Y-n(2+\lambda_2)| \geq \delta|x-2n|-n|\lambda_2|\}\, f_X(x)dx$$

$$= \int_0^\infty \mathbb{P}\left\{\frac{1}{n}|Y-n(2+\lambda_2)| \geq \frac{\delta|x-2n|-n|\lambda_2|}{n}\right\} f_X(x)dx$$

$$= \int_0^\infty \mathbb{P}\left\{\frac{1}{n}\left|\sum_{i=1}^{n}(Y_i-(2+\lambda_2)\right| \geq t_1\right\} f_X(x)dx, \quad \text{where, } t_1 = \frac{\delta|x-2n|-n|\lambda_2|}{n}$$

According to Corrollary 1, we get

$$\mathbb{P}\{|Y-2n| \geq t_1\} \leq \begin{cases} 2.e^{-\frac{nt_1^2}{8(2+2\lambda_2)^2}}, & \text{if } 0 \leq t_1 \leq (2+2\lambda_2)^2, \\ 2.e^{-\frac{nt_1}{8}}, & \text{if } t_1 \geq (2+2\lambda_2)^2, \\ 2, & \text{if } t_1 < 0. \end{cases} \tag{5.20}$$

Case 2: $\mathbb{P}\left\{\left|\frac{Z-2n}{X-2n}\right| \geq \delta\right\}$, where $\delta = \left(\frac{1}{1+\frac{v}{\varepsilon-\left|\alpha_1-\hat{\beta}_1\right|}}\right)^2$.

Following the same line of proof of case 1, we get

$$\mathbb{P}\{|Z-2n| \geq \delta|X-2n|\} \leq \begin{cases} 2.e^{-\frac{nt_2^2}{8(2+2\lambda_3)^2}}, & \text{if } 0 \leq t_2 \leq (2+2\lambda_3)^2, \\ 2.e^{-\frac{nt_2}{8}}, & \text{if } t_2 \geq (2+2\lambda_3)^2, \\ 2, & \text{if } t_2 < 0. \end{cases} \tag{5.21}$$

where, $t_2 = \frac{\delta|x-2n|-n|\lambda_3|}{n}$

Hence, combining (5.20) and (5.21), we get the upper bound of (5.18). A similar technique is used to provide an probability upper bound on the estimate of α_2. Combining both the bounds of α_1 and α_2 we get the required bound of the proposed algorithm. ■

Chapter 6

Numerical Simulations

We estimated the initial value of $(\hat{\beta}_1, \hat{\beta}_2)$. In addition to the LoS path, we assume that there are 4 NLoS paths due to scatters between the user and the LISBT. The elevation and azimuth angles of each NLoS path from those scatters to the center of LISBT follow uniform distribution, i.e., $U(0, 2\pi)$. Moreover, we consider the path coefficient of each NLoS path as a complex Gaussian distribution, i.e., $CN(0, \sigma^2)$, where σ^2 is 20 dB weaker than the power of the LoS component. We considered the far-field case when $d_0 = 200m$. The system parameters for numerical experiments are listed in Table 6.1.

Table 6.1: A list of system parameters for numerical experiments

Parameters	Values	Description
f_c	30 GHz	Carrier frequency
λ	1 cm	Wavelength
L_x	1 m	Width of the RM
L_y	1 m	Length of the RM
d_r	$\lambda/4$	Unit element spacing
L_e	d_r	Width and length of each phase-shifting element
P	30 dBm	Transmission power of the LISBT during data transmission
σ_s^2	-115 dBm	Noise power for 200 KHz

6.0.1 Analysis of Proposed Algorithm

We will try to plot the upper bound of the proposed algorithm in terms of α_1 as $2(\mathbb{P}\{|Y-2n| \geq \delta|X-2n|\} + \mathbb{P}\{|Z-2n| \geq \delta|X-2n|\})$. and compare it with the actual probability given by $\mathbb{P}\{|\hat{\alpha}_1 - \alpha_1|\}$.

In Fig. 6.1 and Fig. 6.2, we show the convergence property of the proposed algorithm for increasing values of $\varepsilon = \{0.02, 0.05, 0.1\}$ for both the parameters α_1 and α_2. We run the simulation for 100 times. We see that for each ε the proposed algorithm converges to 0 as we increase the number of pilots. But we see that for initial small number of samples (< 100), the upper bound of the proposed algorithm is greater than 1.

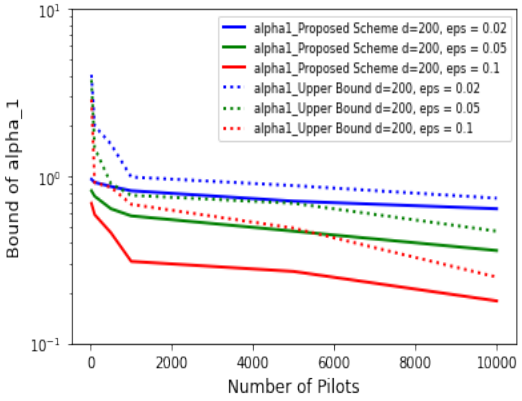

Figure 6.1: Prob. Bound of α_1 v/s Pilots for $\varepsilon = \{0.02, 0.05, 0.1\}$

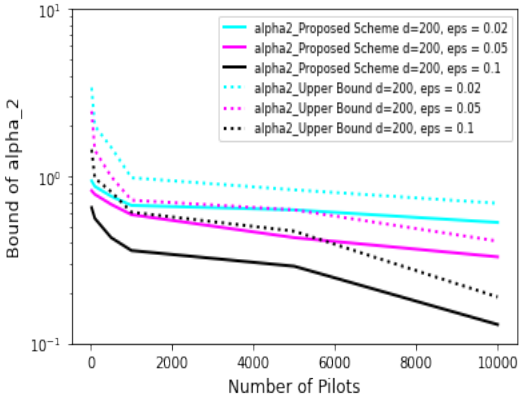

Figure 6.2: Prob. Bound of α_2 v/s Pilots for $\varepsilon = \{0.02, 0.05, 0.1\}$

6.0.2 Compare Proposed Algorithm and Benchmark Scheme

According to the approximated channel model, the received power at the user of LISBT-assisted wireless communication system, denoted by $P_r(\beta_1, \beta_2)$, is given as

$$P_r(\beta) = P_t \left| H^{(ff)}(\beta_1, \beta_2) \right|^2 \tag{6.1}$$

where P_t is the transmission power at the LISBT. The LISBT uses the acquired CSI during the channel estimation period to maximize the received data rate by the user. Therefore, we consider the achieved data rate by the user using the acquired CSI as a performance metric. The achieved data rate is calculated by

$$R = log_2 \left(1 + \frac{Pr}{\sigma^2} \right),$$

where P_r is the received power at the user in (6.1). We applied the two different cases for both far-field ($d_0 = 200m$) and near-field ($d_0 = 10m$). We tried to compare our proposed algorithm with two benchmark, named as Iterative Algorithm (ref. 2) as given in [6]. The paper [6] explains that the Iterative Algorithm (ref. 2)

provides significant gain over the other benchmark schemes, such as, a hierarchical search scheme and a CS-based channel estimation scheme, for far-field since it exploits the specific structure of the radiated beam (the sinc function). The Iterative Algorithm is as follows:

Algorithm 2 Iterative Algorithm: Finding the estimated values for α_1 and α_2 [6]

1: **Initialization:** $k=0$, set $\left(\beta_1^{(0)},\beta_2^{(0)}\right)$ to a random pair between $[-1,1]$.
2: **while** convergence==False **do**
3: $k=k+1$ and obtain $\hat{\alpha}_1$ and $\hat{\alpha}_2$ by (6.2) and (6.3).
4: Update $\left(\beta_1^{(k)},\beta_2^{(k)}\right)$ by $(\hat{\alpha}_1,\hat{\alpha}_2)$.
5: **if** $\left(\beta_1^{(k)}-\beta_1^{(k-1)}\right)^2+\left(\beta_2^{(k)}-\beta_2^{(k-1)}\right)^2<\delta$, or $k>K_max$ **then**
6: convergence = True
7: **end if**
8: **end while**
9: **Output:** $\alpha_1=\beta_1^{(k)},\alpha_2=\beta_2^{(k)}$.

In the k-th iteration,

$$\alpha_1^{(1)/(2)}=\beta_1^{(k-1)}+\frac{r\left(\beta_1^{(k-1)}+v,\beta_2^{(k-1)}\right)}{r\left(\beta_1^{(k-1)}+v,\beta_2^{(k-1)}\right)\pm r\left(\beta_1^{(k-1)},\beta_2^{(k-1)}\right)}$$

$$\alpha_1^{(3)/(4)}=\beta_1^{(k-1)}+\frac{r\left(\beta_1^{(k-1)}-v,\beta_2^{(k-1)}\right)}{-r\left(\beta_1^{(k-1)}-v,\beta_2^{(k-1)}\right)\pm r\left(\beta_1^{(k-1)},\beta_2^{(k-1)}\right)}$$

where v is selected such that $K_x v\in\mathbb{N}$. We obtain the estimated α_1 as the average of two answers with the minimum difference.

$$\hat{\alpha}_1=\left\{\frac{\alpha_1^{(i)}+\alpha_1^{(j)}}{2}:\min_{i,j}\left|\alpha_1^{(i)}-\alpha_1^{(j)}\right|;i\in\{1,2\},j\in\{3,4\}\right\} \tag{6.2}$$

$$\alpha_2^{(1)/(2)}=\beta_2^{(k-1)}+\frac{r\left(\beta_1^{(k-1)},\beta_2^{(k-1)}+w\right)}{r\left(\beta_1^{(k-1)},\beta_2^{(k-1)}+w\right)\pm r\left(\beta_1^{(k-1)},\beta_2^{(k-1)}\right)}$$

$$\alpha_2^{(3)/(4)}=\beta_2^{(k-1)}+\frac{r\left(\beta_1^{(k-1)},\beta_2^{(k-1)}-w\right)}{-r\left(\beta_1^{(k-1)},\beta_2^{(k-1)}-w\right)\pm r\left(\beta_1^{(k-1)},\beta_2^{(k-1)}\right)}$$

where w is selected such that $K_y w \in \mathbb{N}$. We obtain the estimated α_2 as the average of two answers with the minimum difference.

$$\hat{\alpha_2} = \left\{ \frac{\alpha_2^{(i)} + \alpha_2^{(j)}}{2} : \min_{i,j} \left| \alpha_2^{(i)} - \alpha_2^{(j)} \right| ; i \in \{1,2\}, j \in \{3,4\} \right\} \tag{6.3}$$

In Fir. 6.3 we compared the achievable rates of the proposed scheme and benchmark schemes, as given by Iterative Algorithm (refer Algorithm 2) and the oracle scheme where α_1 and α_2 are estimated accurately and achieved the maximum rate. We considered both far-field (i.e. $d = 200m$) and near-field ((i.e. $d = 10m$) regions of the LISBT with respect to the transmit power of the pilot signals when the number of the pilot signals is fixed to 23. For all the algorithms we used same number of 23 pilots for both far-field and near-field. We run the simulation for 100 times. We see that the achievable rates of far-field is lower than the near-field as the user is far from the LISBT and hence the data rate decreases significantly. However, for both far-field and near-field we see that the proposed Algorithm 1 gives higher rates than other two benchmark schemes.

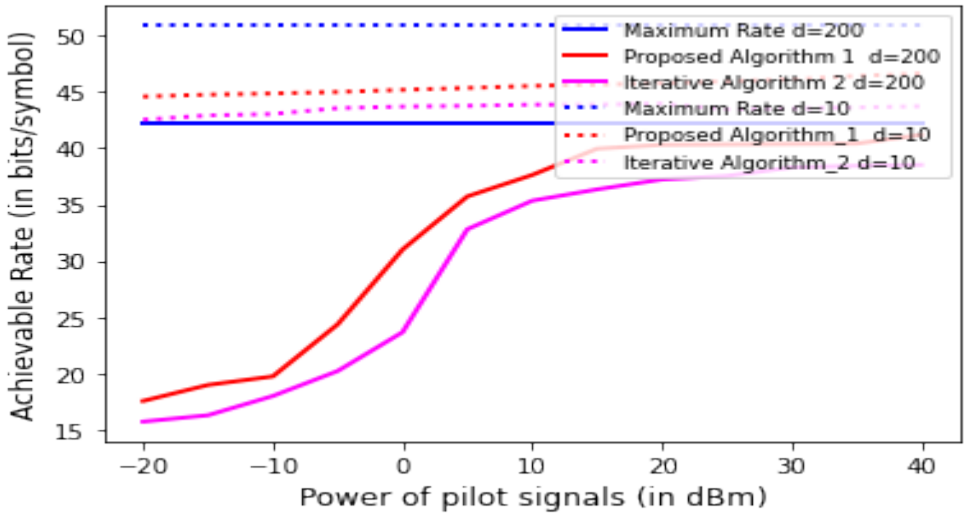

Figure 6.3: Achievable rate vs. the transmit power of the pilot signals (in dBm).

Chapter 7

Conclusion

In this paper, we proposed a channel estimation scheme for the LISBT-assisted wireless communication system. In the far-field region of the LISBT, we modeled the channel based on the path parameters of the system. It is shown that only two path parameters are required to be estimated to obtain the optimal phase shifts for all phase-shifting elements of the LISBT. We showed that the proposed scheme requires only five pilots to perfectly estimate the unknown parameters in the absence of noise. In the presence of the noise, an iterative algorithm was presented to estimate the unknown path parameters. The simulation results verified that the proposed scheme achieves significant performance gains over existing channel estimation schemes.

Bibliography

[1] Alekh Agarwal, Dean P Foster, Daniel J Hsu, Sham M Kakade, and Alexander Rakhlin. Stochastic convex optimization with bandit feedback. *Advances in Neural Information Processing Systems*, 24:1035–1043, 2011.

[2] Mustafa Riza Akdeniz, Yuanpeng Liu, Mathew K Samimi, Shu Sun, Sundeep Rangan, Theodore S Rappaport, and Elza Erkip. Millimeter wave channel modeling and cellular capacity evaluation. *IEEE journal on selected areas in communications*, 32(6):1164–1179, 2014.

[3] Kangjian Chen and Chenhao Qi. Beam training based on dynamic hierarchical codebook for millimeter wave massive mimo. *IEEE Communications Letters*, 23(1):132–135, 2018.

[4] Fei Dai and Jie Wu. Efficient broadcasting in ad hoc wireless networks using directional antennas. *IEEE Transactions on Parallel and Distributed Systems*, 17(4):335–347, 2006.

[5] Davide Dardari. Communicating with large intelligent surfaces: Fundamental limits and models. *IEEE Journal on Selected Areas in Communications*, 38(11):2526–2537, 2020.

[6] Mojtaba Ghermezcheshmeh, Vahid Jamali, Haris Gacanin, and Nikola Zlatanov. Channel estimation for large intelligent surface-based transceiver using a parametric channel model. *arXiv preprint arXiv:2112.02874*, 2021.

[7] Ali Grami. *Introduction to digital communications*. Academic Press, 2015.

[8] Chongwen Huang, Sha Hu, George C Alexandropoulos, Alessio Zappone, Chau Yuen, Rui Zhang, Marco Di Renzo, and Merouane Debbah. Holographic mimo surfaces for 6g wireless networks: Opportunities, challenges, and trends. *IEEE Wireless Communications*, 27(5):118–125, 2020.

[9] Vahid Jamali, Antonia M Tulino, Georg Fischer, Ralf R Müller, and Robert Schober. Intelligent surface-aided transmitter architectures for

millimeter-wave ultra massive mimo systems. *IEEE Open Journal of the Communications Society*, 2:144–167, 2020.

[10] Stephan Kunne, Lorenzo Maggi, Johanne Cohen, and Xinneng Xu. Anytime backtrack unimodal bandits and applications to cloud computing. In *2020 IFIP Networking Conference (Networking)*, pages 82–90. IEEE, 2020.

[11] Khaled B Letaief, Wei Chen, Yuanming Shi, Jun Zhang, and Ying-Jun Angela Zhang. The roadmap to 6g: Ai empowered wireless networks. *IEEE Communications Magazine*, 57(8):84–90, 2019.

[12] Stefan Magureanu, Richard Combes, and Alexandre Proutiere. Lipschitz bandits: Regret lower bound and optimal algorithms. In *Conference on Learning Theory*, pages 975–999. PMLR, 2014.

[13] Walid Saad, Mehdi Bennis, and Mingzhe Chen. A vision of 6g wireless systems: Applications, trends, technologies, and open research problems. *IEEE network*, 34(3):134–142, 2019.

[14] Krishnasamy T Selvan and Ramakrishna Janaswamy. Fraunhofer and fresnel distances: Unified derivation for aperture antennas. *IEEE Antennas and Propagation Magazine*, 59(4):12–15, 2017.

[15] Nir Shlezinger, George C Alexandropoulos, Mohammadreza F Imani, Yonina C Eldar, and David R Smith. Dynamic metasurface antennas for 6g extreme massive mimo communications. *IEEE Wireless Communications*, 28(2):106–113, 2021.

[16] Martin J Wainwright. *High-dimensional statistics: A non-asymptotic viewpoint*, volume 48. Cambridge University Press, 2019.

[17] Ziwei Wan, Zhen Gao, Feifei Gao, Marco Di Renzo, and Mohamed-Slim Alouini. Terahertz massive mimo with holographic reconfigurable intelligent surfaces. *IEEE Transactions on Communications*, 2021.

[18] Qingqing Wu and Rui Zhang. Intelligent reflecting surface enhanced wireless network via joint active and passive beamforming. *IEEE Transactions on Wireless Communications*, 18(11):5394–5409, 2019.

[19] Qingqing Wu, Shuowen Zhang, Beixiong Zheng, Changsheng You, and Rui Zhang. Intelligent reflecting surface aided wireless communications: A tutorial. *IEEE Transactions on Communications*, 2021.

[20] Henk Wymeersch, Jiguang He, Benoit Denis, Antonio Clemente, and Markku Juntti. Radio localization and mapping with reconfigurable intelligent surfaces: Challenges, opportunities, and research directions. *IEEE Vehicular Technology Magazine*, 15(4):52–61, 2020.

[21] Zhenyu Xiao, Tong He, Pengfei Xia, and Xiang-Gen Xia. Hierarchical codebook design for beamforming training in millimeter-wave communication. *IEEE Transactions on Wireless Communications*, 15(5):3380–3392, 2016.

[22] Jianjun Zhang, Yongming Huang, Qingjiang Shi, Jiaheng Wang, and Luxi Yang. Codebook design for beam alignment in millimeter wave communication systems. *IEEE Transactions on Communications*, 65(11):4980–4995, 2017.

[23] Feibai Zhu, An Liu, and Vincent KN Lau. Channel estimation and localization for mmwave systems: A sparse bayesian learning approach. In *ICC 2019-2019 IEEE International Conference on Communications (ICC)*, pages 1–6. IEEE, 2019.